



# HHS Public Access

Author manuscript

*Acc Chem Res.* Author manuscript; available in PMC 2022 September 17.

Published in final edited form as:

*Acc Chem Res.* 2021 July 06; 54(13): 2844–2857. doi:10.1021/acs.accounts.1c00185.

## Seeking Illumination: The Path to Chemiluminescent 1,2-Dioxetanes for Quantitative Measurements and *In Vivo* Imaging

**Uroob Haris<sup>†</sup>,**

Department of Chemistry, Southern Methodist University, Dallas, Texas 75275-0314, United States

**Husain N. Kagalwala<sup>†</sup>,**

Department of Chemistry, Southern Methodist University, Dallas, Texas 75275-0314, United States

**Yujin Lisa Kim,**

Department of Chemistry, Southern Methodist University, Dallas, Texas 75275-0314, United States

**Alexander R. Lippert**

Department of Chemistry, Southern Methodist University, Dallas, Texas 75275-0314, United States

### CONSPECTUS:

Chemiluminescence is a fascinating phenomenon that evolved in nature and has been harnessed by chemists in diverse ways to improve life. This Account tells the story of our research group's efforts to formulate and manifest spiroadamantane 1,2-dioxetanes with triggerable chemiluminescence for imaging and monitoring important reactive analytes in living cells, animals, and human clinical samples. Analytes like reactive sulfur, oxygen and nitrogen species, as well as pH and hypoxia can be indicators of cellular function or dysfunction and are often implicated in the causes and effects of disease. We begin with a foundation in binding-based and activity-based fluorescence imaging that has provided transformative tools for understanding biological systems. The intense light sources required for fluorescence excitation, however, introduce autofluorescence and light scattering that reduces sensitivity and complicates *in vivo* imaging. Our work and the work of our collaborators were the first to demonstrate that spiroadamantane 1,2-dioxetanes had sufficient brightness and biological compatibility for *in vivo* imaging of enzyme activity and reactive analytes like hydrogen sulfide (H<sub>2</sub>S) inside of living mice. This launched an era of renewed interest in 1,2-dioxetanes that has resulted in a plethora of new chemiluminescence imaging agents developed by groups around the world. Our own

---

**Corresponding Author: Alexander R. Lippert** – Department of Chemistry, Southern Methodist University, Dallas, Texas 75275-0314, United States; alippert@smu.edu.

<sup>†</sup>U.H. and H.N.K. contributed equally.

Author Contributions

The manuscript was written through contributions of all authors. All authors have given approval to the final version of the manuscript.

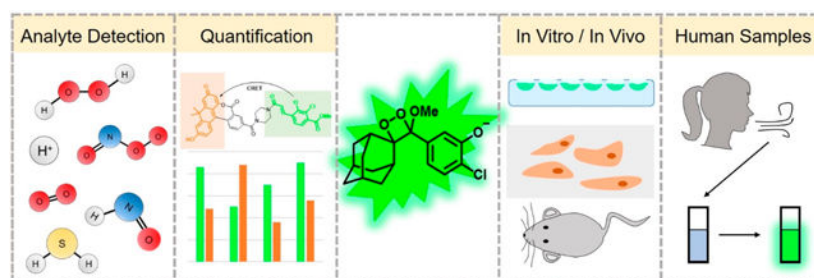
Notes

The authors declare the following competing financial interest(s): A.R.L. declares a financial stake in BioLum Sciences.

Complete contact information is available at: <https://pubs.acs.org/10.1021/acs.accounts.1c00185>

research group focused its efforts on reactive sulfur, oxygen, and nitrogen species, pH, and hypoxia, resulting in a large family of bright chemiluminescent 1,2-dioxetanes validated for cell monitoring and *in vivo* imaging. These chemiluminescent probes feature low background and high sensitivity that have been proven quite useful for studying signaling, for example, the generation of peroxynitrite ( $\text{ONOO}^-$ ) in cellular models of immune function and phagocytosis. This high sensitivity has also enabled real-time quantitative reporting of oxygen-dependent enzyme activity and hypoxia in living cells and tumor xenograft models. We reported some of the first ratiometric chemiluminescent 1,2-dioxetane systems for imaging pH and have introduced a powerful kinetics-based approach for quantification of reactive species like azanone (nitroxyl,  $\text{HNO}$ ) and enzyme activity in living cells. These tools have been applied to untangle complex signaling pathways of peroxynitrite production in radiation therapy and as substrates in a split esterase system to provide an enzyme/substrate pair to rival luciferase/luciferin. Furthermore, we have pushed chemiluminescence toward commercialization and clinical translation by demonstrating the ability to monitor airway hydrogen peroxide in the exhaled breath of asthma patients using transiently produced chemiluminescent 1,2-dioxetanedione intermediates. This body of work shows the powerful possibilities that can emerge when working at the interface of light and chemistry, and we hope that it will inspire future scientists to seek out ever brighter and more illuminating ideas.

## Graphical Abstract



## 1. INTRODUCTION

Molecular imaging in living cells and animals provides a powerful approach to illuminate complex chemical processes that underlie biological phenomena. Binding-based and activity-based imaging have emerged as two dominant approaches for molecular imaging.<sup>5-7</sup> Binding-based imaging relies on linking supramolecular recognition units to fluorophores such that fluorescence emission is modulated, usually based on a photoinduced electron or energy transfer (PeT or PET, respectively) quenching mechanism.<sup>8</sup> Activity-based or reaction-based sensing relies on making or breaking covalent bonds to modulate a response, often mediated by a self-immolative linker design.<sup>9</sup> These approaches have been widely applied to study cellular signaling of metal ions and cellular parameters including calcium,<sup>10</sup> zinc,<sup>11,12</sup> magnesium,<sup>13</sup> potassium,<sup>14</sup> copper,<sup>15</sup> iron,<sup>16</sup> pH,<sup>17</sup> chloride,<sup>18,19</sup> and voltage.<sup>20</sup> Reactive sulfur, oxygen, and nitrogen (RSO) species are a class of signaling molecules that can rapidly diffuse and whose signaling properties rely on their chemical reactivity. Due to this reactive nature, reaction-based approaches are ideally poised to study these molecules.<sup>21,22</sup> These species rapidly interact with each other to form a super family of signaling molecules and aberrant species referred to as the reactive species interactome.<sup>23</sup>

Fluorescent probe strategies have been implemented for reactive oxygen species like hydrogen peroxide ( $\text{H}_2\text{O}_2$ ) and peroxyxynitrite ( $\text{ONOO}^-$ ),<sup>22,24–26</sup> reactive nitrogen species like nitric oxide (NO) and azanone (nitroxyl, HNO),<sup>22,27</sup> reactive sulfur species like hydrogen sulfide ( $\text{H}_2\text{S}$ ) and polysulfides ( $\text{RS}_n\text{H}/\text{RS}_n\text{R}$ ),<sup>21,22,28–30</sup> reactive carbon species like formaldehyde ( $\text{CH}_2\text{O}$ ) and carbon monoxide (CO),<sup>31,32</sup> and oxygen ( $\text{O}_2$ )/hypoxia.<sup>33</sup> Given the complexity of their interactions, dual-responsive probes that react with multiple species are being explored as an enticing solution to this problem.<sup>34,35</sup> While promising, fluorescence-based methods inherently suffer from light scattering and autofluorescence, which pose some limitations on sensitivity and whole animal imaging.

Chemiluminescence is now emerging as a powerful molecular imaging approach to address these limitations. This area has exploded recently due to demonstrations of *in vivo* compatibility<sup>1,36</sup> and the advent of innovative chemiluminescent 1,2-dioxetane designs by Shabat and co-workers.<sup>37,38</sup> Triggered emission from spiroadamantane 1,2-dioxetanes was first developed by Schaap and co-workers,<sup>39–41</sup> and these dioxetanes found commercial application for *in vitro* research purposes. The mechanism of chemiluminescence emission has been extensively studied, but it is still incompletely understood.<sup>42</sup> It is thought to proceed via a chemically initiated electron exchange luminescence (CIEEL) mechanism with a solvent-cage back electron transfer step as evidenced by a viscosity dependence on the luminescence emission intensity (Scheme 1).<sup>43,44</sup> An odd/even effect on the position of the dioxetane has been observed, although the root cause of this effect remains to be completely elucidated.<sup>45,46</sup> We direct the reader to other excellent recent review articles<sup>47–49</sup> for expanded current and historical perspectives. This Account will focus on research from our own laboratory on the use of chemiluminescent dioxetanes for imaging RSON species, pH, and hypoxia in living organisms, with an emphasis on quantitative methods and application in mammalian cell culture and *in vivo* mouse models. This work has resulted in a diverse family of bright chemiluminescent 1,2-dioxetanes (Figure 1).

## 2. REACTION-BASED APPROACHES FOR STUDYING REACTIVE SULFUR, OXYGEN, AND NITROGEN SPECIES

Reaction-based probes are increasingly being used as sensitive imaging agents for small molecules which are fleeting in nature and similar in shape and size, with reactive species like hydrogen sulfide ( $\text{H}_2\text{S}$ ), peroxyxynitrite ( $\text{ONOO}^-$ ), and azanone (HNO) being prime examples. Our laboratory has been interested in exploiting the specific reactivity of such biologically active small molecules to develop reactivity-based responsive reporters that do not depend on noncovalent binding of substrates.

One such class of reaction-based fluorescent probes was the azide-based SF series of probes for direct, endogenous, real-time detection of  $\text{H}_2\text{S}$ ,<sup>50</sup> a reactive small molecule with wide-ranging roles in mammalian physiology.<sup>51–54</sup> In response to  $\text{H}_2\text{S}$ , the fluorophore is unmasked and fluorescence turn-on is observed. SF7-AM,<sup>55</sup> the cell-trappable variant in the SF series (Figure 2A), was shown to detect endogenous  $\text{H}_2\text{S}$  production in human umbilical vein endothelial cells (HUVECs) when stimulated with vascular endothelial growth factor (VEGF). The study also employed SF7-AM to investigate enzymatic pathways that lead to

VEGF-triggered H<sub>2</sub>S production. Treatment of VEGF-dosed HUVECs with inhibitors for cystathionine  $\gamma$ -lyase (CSE), VEGF Receptor 2 (VEGFR2), and H<sub>2</sub>O<sub>2</sub>-generating NADPH-oxidase (Nox), led to decreased SF7-AM turn-on, thus establishing the dependence of VEGF-stimulated H<sub>2</sub>S generation on CSE, VEGFR2, and Nox-derived H<sub>2</sub>O<sub>2</sub> (Figure 3).

Following this blueprint, our group capitalized on expertise in chemoselective reaction design<sup>56</sup> and began its exploration of sensors to detect small molecules, particularly RSON and carbon species. To observe generation of acetaldehyde from ethanol and alcohol dehydrogenase in lung epithelial cells, we designed reaction-based probe acetaldehydefluor-1 (AF1),<sup>57</sup> utilizing a condensation reaction between reactive carbonyls and a hydrazinyl naphthalimide based scaffold with quenched fluorescence to induce fluorescence turn-on (Figure 2B). For direct detection of the biological oxidant peroxynitrite (ONOO<sup>-</sup>)<sup>58</sup> we developed a magnetic resonance probe leveraging a newly discovered ONOO<sup>-</sup> promoted oxidative decarbonylation reaction of fluoroisatin  $\alpha$ -ketocarboxyls (Figure 2C).<sup>59</sup> Formation of the fluoroanthranilic acid product was monitored using <sup>19</sup>F NMR spectroscopy. Though these techniques enabled direct imaging/detection of acetaldehyde and peroxynitrite in cells, we still aspired to develop a more sensitive and dynamic imaging system that could report on analyte fluxes from within tissue and even in whole animals.

### 3. ESTABLISHING CHEMILUMINESCENT 1,2-DIOXETANES FOR *IN VIVO* IMAGING

Excited state emitters for chemiluminescence are generated via a chemical reaction as opposed to light excitation for fluorescence.<sup>42</sup> Therefore, chemiluminescence imaging is not as impeded by autofluorescence and light scattering, significantly improving sensitivity of this imaging method over fluorescence imaging and affording higher tissue penetration and imaging depth. Since chemiluminescence outputs transient light emission, signal can be detected as it is generated, enabling dynamic imaging and interception of transient species. Despite these obvious advantages, there was great uncertainty about the compatibility of triggerable 1,2-dioxetanes with living systems. Would these compounds be bright enough to be observable through living tissue? Could they generate enough flux upon reaction with small molecule analytes? Would living animals tolerate these compounds physiologically?

In an important study by Liu and Mason in 2010,<sup>36</sup> spiroadamantane 1,2-dioxetanes were first shown to be viable as *in vivo* reporters of enzymatic activity in live mice. A commercially available Galacto-Light Plus microplate-based chemiluminescence assay (Figure 4A) was adapted for *in vivo* use to image  $\beta$ -galactosidase enzymatic activity in transgenic mice growing LacZ tumors for overexpression of  $\beta$ -galactosidase. The components of this packaged assay, a 1,2-dioxetane with a  $\beta$ -D-galacto pyranoside trigger (Galacton Plus) and Emerald enhancer were administered via intravenous and intratumor injection in live mice growing LacZ tumors. Chemiluminescence light emission was observed within 10 s of injection using an IVIS Spectrum light detection instrument, and up to 10-fold differences in emission intensity were observed between LacZ tumors and wildtype tumors. These studies demonstrated two key points. First, light emission from

spiroadamantane 1,2-dioxetanes was sufficient for noninvasive *in vivo* imaging through animal tissue and second, high-turnover enzymatic reactions could be observed using these probes.

Inspired by this demonstration of sensitive *in vivo* chemiluminescence imaging, we sought to explore whether spiroadamantane 1,2-dioxetanes could be used with reaction-based approaches for imaging small molecule reactive analytes in living animals. We designed reaction-based first-generation chemiluminescent H<sub>2</sub>S probes CHS-1, -2, and -3 for *in vivo* detection of H<sub>2</sub>S.<sup>1</sup> A *para*-azidobenzyl carbonate trigger attached to a sterically stabilized spiroadamantane 1,2-dioxetane results in light emission upon H<sub>2</sub>S-mediated azide reduction and consequent self-immolative cleavage to the excited state phenolate. A comparative study of emission response between CHS-1, -2, and -3, differing in structure by the substituent (H, F, or Cl) ortho to the phenolate, showed that emission intensity at pH 7.4 increases with phenol acidity: the chloro-substituted CHS-3 showed highest turn-on response under physiological conditions. CHS-3 with the Emerald II enhancer was able to detect differences in H<sub>2</sub>S in A549 lung epithelial cells produced in response to addition of homocysteine, a substrate for H<sub>2</sub>S-generating enzyme cystathionine  $\gamma$ -lyase (CSE), and propargylglycine, a CSE inhibitor. Most significantly, we established that chemiluminescent 1,2-dioxetane based probes could be used for *in vivo* detection of small molecules such as hydrogen sulfide; CHS-3 exhibited a four times stronger chemiluminescent response when injected into the intraperitoneal cavity of live mice with H<sub>2</sub>S donor sodium sulfide (Na<sub>2</sub>S) as compared to a vehicle control (Figure 4B). This was the first demonstration that reactive species could be imaged *in vivo* using 1,2-dioxetane probes.

Following successful *in vivo* chemiluminescence imaging using CHS-3, we focused on designing a chemiluminescent probe that could report on tissue oxygenation in living animals.<sup>60</sup> Tumor tissue is characteristically hypoxic owing to its irregular vasculature, and imaging this hypoxia in the tumor microenvironment can provide insight about tumor growth, metastasis, and response to therapy.<sup>33</sup> We based our hypoxia chemiluminescent (HyCL) probes on oxygen-dependent enzymatic reduction of a nitroaromatic trigger, with the aim of developing an inexpensive tumor imaging method. Though HyCL-1 and HyCL-2 both showed a sensitive dose-dependent response to nitroreductase, HyCL-2, which incorporates an ether linkage between the 1,2-dioxetane scaffold and the *para*-nitrobenzyl trigger, was determined to have lower background emission and higher selectivity than the carbonate-linked HyCL-1 (Figure 5A). We conducted studies to establish that HyCL-2 can image different oxygen levels *in vitro* in aerated, oxygenated, and deoxygenated buffers and further demonstrated its ability to image tumor oxygenation *in vivo* in transgenic mice grafted with human lung tumors. Intratumoral injection of HyCL-2 with enhancer in mice when inhaling air containing 21% oxygen resulted in higher chemiluminescence emission than when switched to 100% oxygen, showing that HyCL-2 can report on tissue oxygenation levels *in vivo* (Figure 5B).

#### 4. OPENING A GATEWAY TO ENHANCER FREE IMAGING

Although the 1,2-dioxetane chemiluminescent probes discussed thus far provided us with vital information on their use in biological systems, efficient imaging with these probes

relied on the use of polymeric enhancer solutions to prevent luminescence quenching and to enable red-shifted emission. Our laboratory had been exploring energy transfer approaches to overcome this obstacle and had synthesized constructs such as a through-bond energy transfer cassette. During our ongoing work, however, an exciting development in the field of 1,2-dioxetane-based chemiluminescent probes was reported by Green, Eilon, Hananya, Shabat, and co-workers.<sup>37,38</sup> They found that a relatively simple modification of the phenol-benzoate ring with an electron-withdrawing methyl acrylate or acrylonitrile group *ortho* to the phenol led to large increases in chemiluminescence quantum yield under aqueous conditions (Figure 6). Moreover, a red-shifted chemiluminescence emission was attained, making these structures more relevant for biological applications. This work paved the way for further development of analyte-specific direct chemiluminescent probes and certainly enriched the efforts from our own laboratory.

In 2018, our laboratory reported a reaction-based chemiluminescent probe, PNCL, for direct cellular detection of peroxynitrite (ONOO<sup>-</sup>).<sup>2</sup> Armed with knowledge from our earlier work on an <sup>19</sup>F magnetic resonance probe for ONOO<sup>-</sup>, we envisioned attaching an isatin moiety as a reaction handle to a 1,2-dioxetane chemiluminescent scaffold to leverage the peroxynitrite-mediated oxidative decarbonylation reaction and induce chemiluminescence. Studies performed *in vitro* revealed the ability of PNCL to monitor ONOO<sup>-</sup> fluxes over time, to demonstrate dose dependence, and to selectively detect ONOO<sup>-</sup> over a multitude of biological relevant cations, RSON species and radical byproducts. Most importantly, PNCL showed low toxicity in living cells and detected ONOO<sup>-</sup> generated by donor compounds like SIN-1 across multiple cell lines, as well as ONOO<sup>-</sup> produced by macrophages stimulated by lipopolysaccharide (LPS) (Figure 7). This study demonstrated that PNCL could serve as a promising tool to identify ONOO<sup>-</sup> in both chemical and biological systems without addition of signal enhancer.

## 5. QUANTIFICATION USING CHEMILUMINESCENT 1,2-DIOXETANES

Following sustained success with small molecule chemiluminescence imaging in living systems, we turned our attention to precise quantification of these analytes, which can be challenging due to experimental fluctuations. Ratiometric imaging,<sup>61</sup> wherein emission intensity at multiple wavelengths is monitored, offered a solution. Ratiometric responses are less sensitive to experimental variables and thus allow a more accurate quantification of analytes important in health and disease such as pH.<sup>62,63</sup> While fluorescent ratiometric probes for pH imaging are well-known,<sup>64-67</sup> their chemiluminescent 1,2-dioxetane counterparts are quite rare.

Our initial strategy involved inducing an energy transfer cascade between chemiluminescence emission from a spiroadamantane 1,2-dioxetane and a pH sensitive dye, carboxy SNARF-1 via a Sapphire II or Emerald II enhancer (Scheme 2).<sup>68</sup> Carboxy SNARF-1 exhibits pH dependent emissions at 585 and 650 nm, the relative intensities being determined by the ratio of the protonated and deprotonated forms, respectively. The peak at 650 nm was found to increase more rapidly with an increase in pH due to increased concentration of the deprotonated form. A ratiometric pH dependent plot could thus be generated by plotting the ratio of emission intensities at 650 and 585 nm, depicting a greater

than 5-fold increase in chemiluminescence signal in response to pH over a range of 6–10. We conducted additional studies to show that this ratiometric pH quantification could be achieved in complex biological medium such as fetal bovine serum and established this system to be compatible with IVIS Spectrum imaging when using 580 and 640 nm filters.

Having successfully demonstrated ratiometric pH quantification using the principle of energy transfer between multiple components, we focused on probes that could be more viable for *in vivo* applications. In 2020, we reported Ratio-pHCL-1, a single molecule ratiometric chemiluminescence resonance energy transfer (CRET) sensor for *in vivo* pH imaging (Figure 8).<sup>4</sup> Here, we conjugated an acrylate modified spiroadamantane 1,2-dioxetane moiety to a pH sensitive carbofluorescein dye via a piperazine linker. Upon being subjected to aqueous pH buffers, energy transfer from the chemiluminescent phenolate ( $\lambda_{em} = 530$  nm) to the carbofluorescein ( $\lambda_{em} = 580$  nm) occurs, with the latter peak increasing more rapidly with pH due to increased concentration of the ring-opened carbofluorescein, allowing for ratiometric measurements (Figure 8A). Ratio-pHCL-1 provided consistent measurements of pH over a biologically relevant range of 6.8–8.4, and the ratiometric response was independent of most common confounding variables. Interestingly, placing a 2.8 mm thick slice of bologna over the reaction well-plate did not hamper the ratiometric response, providing strong evidence of signal tissue penetration. Intraperitoneal injections in live mice with Ratio-pHCL-1 generated flux outputs of more than  $10^8$ – $10^9$  photons/s (Figure 8B), and as with *in vitro* experiments an increase in flux ratio with increasing pH was observed *in vivo* (Figure 8C).

While ratiometric approaches have been well-validated for the quantification of metal ions using probes with rapid rates of binding<sup>69,70</sup> or in a reaction-based approach with fast forward and reverse equilibrium reactions,<sup>71–73</sup> applying this approach to small molecule reactive analytes and enzymes faces steep obstacles. To be useful for quantification, reaction-based ratiometric approaches must use a fast and reversible reaction to ensure equilibration of the starting material and product. Given these challenges, we have introduced an alternative to ratiometric imaging that we refer to as a kinetics-based approach that capitalizes on the high sensitivity of chemiluminescence to enable quantification by accurate modeling of the probe kinetics. This approach is analogous to how quantification is achieved using analyte-selective electrodes,<sup>74</sup> and its application to reaction-based probes is very much underexplored.

To investigate a kinetics-based small molecule quantification approach via chemiluminescence, we devised the probe HNOCL-1 for detection of azanone (nitroxyl, HNO),<sup>3</sup> a reactive nitrogen species that has been shown to reduce pain in animal models and can potentially be used for treatment of congestive heart failure.<sup>75</sup> HNOCL-1 contains a triarylphosphine trigger which forms an intermediate azaylide and decomposes to generate chemiluminescence in response to HNO (Figure 9). HNOCL-1 showed high selectivity, a dose-dependent response, and up to 833-fold turn-on when interrogated with the HNO donor, Angeli's salt. With emphasis on quantification, we carried out kinetic modeling and derived a rate expression in terms of the phenol concentration (Figure 9A) with two rate constants:  $k_1$ , the observed second order rate constant of the probe, and  $k_3$ , the rate of chemiluminescent decomposition of the dioxetane. These rate constants were

measured and the derived equation for concentration was used to successfully convert the raw chemiluminescence data into actual picomolar HNO concentrations produced from the reaction of H<sub>2</sub>S with nitric oxide (Figure 9B, C). Furthermore, we demonstrated that HNOCL-1 can track real-time HNO production from both Angeli's salt and the reduction chemistry between the NO donor DEA NONOate and Na<sub>2</sub>S in live cells, with negligible cellular toxicity up to 100 mM HNOCL-1. Finally, HNO imaging in live mice was achieved via intraperitoneal injection of the probe and Angeli's salt. We believe that this work, in principle, can be applied to any reactive species if careful considerations of kinetics and calibrations are performed.

Another example of kinetics-based quantification from our laboratory builds on our earlier work with chemiluminescent hypoxia probes. We designed HyCL-3 and HyCL-4-AM with nitrobenzyl triggers attached to a 1,2-dioxetane scaffold via ether linkage, HyCL-4-AM, containing an acetomethoxy ester, and HyCL-3 with an acrylonitrile group (Figure 10).<sup>76</sup> While both probes displayed high selectivity for oxygen-dependent enzymatic reduction of the nitroaromatic group, the better cellular uptake of HyCL-4-AM resulted in enhanced sensitivity to nitroreductase (NTR) and in appropriate mammalian hypoxia models. HyCL-4-AM was able to distinguish between hypoxic (1% O<sub>2</sub>) and normoxic (20% O<sub>2</sub>) conditions in living A549 cells (Figure 10 B, C) and a kinetic model was devised based on cellular data, which fit well using two rate constants:  $k_1$ , which determines the cellular uptake and ester cleavage, and  $k_2$  which is limited by the nitroaromatic reduction and consequently is sensitive to O<sub>2</sub> levels (Figure 10A). After devising this model for kinetic quantification, we used HyCL-4-AM to image and kinetically quantify hypoxia in tumor xenograft models as well as to measure differences between hypoxic tumors and healthy oxygenated tissues *in vivo* (Figure 10D), demonstrating its applicability for tumor imaging.

## 6. BIOLOGICAL MEASUREMENTS AND APPLICATIONS

In addition to developing chemiluminescent probes for reactive species and analytes, a significant motivation of our laboratory has been to establish the efficacy of both chemiluminescent and fluorescent probes for studying biological interactions and to develop diagnostic procedures and devices for human studies.

In a collaborative study with the Haimotz-Friedman group, we used PNCL to study peroxyxynitrite levels in cells to elucidate the effects of radiation on oxidative stress levels and the role of phosphodiesterase-5 inhibitor sildenafil, *i.e.*, Viagra, in reducing this oxidative stress (Figure 11).<sup>77</sup> Our results shed light on the vascular aspects of postradiotherapy erectile dysfunction and supported previous work which showed that sildenafil helps to preserve erectile function in prostate cancer patients undergoing radiotherapy.<sup>78–80</sup>

We also developed chemiluminescent reporter Chemilum-CM to complement a BS2 split-esterase system for monitoring cellular protein–protein interactions (Figure 12A).<sup>81</sup> The ester-masked probe generated chemiluminescence response upon rapamycin-induced assembly of the esterase within cells, showing increasing chemiluminescence with increasing rapamycin concentration and incubation time (Figure 12B).



## 7. IN HUMAN AND CLINICAL STUDIES

An important thrust of our laboratory's efforts has been toward translating triggered chemiluminescence into clinical and commercial applications. In one such venture, we developed a point-of-care diagnostic chemiluminescent assay for monitoring airway H<sub>2</sub>O<sub>2</sub>, consisting of a 1,2-dioxetanedione mediated peroxyoxalate chemiluminescence system, a smartphone camera, and a home-built dark-box (Figure 13A, B).<sup>82</sup> H<sub>2</sub>O<sub>2</sub> levels in exhaled breath condensate (EBC) samples from human volunteers determined using this platform were found to be in close agreement with the commercial Amplex Red assay. In collaboration with the start-up company BioLum Sciences LLC, we recently evolved our chemiluminescent airway H<sub>2</sub>O<sub>2</sub> quantification platform into the BioSense 2.0 Laboratory module, a stand-alone photon detection device consisting of a photodiode, a 3D-printed adapter for disposable cuvettes, and a Bluetooth 4.0 data transmission module (Figure 13A, C).<sup>83</sup> Using this device, we studied the relationship between airway H<sub>2</sub>O<sub>2</sub> and asthma in EBC samples from 60 adults. Our results agreed with earlier literature showing trends of higher H<sub>2</sub>O<sub>2</sub> in asthma patients as compared to nonasthmatic patients.

We have also used the fluorescent probe Sulfidefluor-4 to quantify H<sub>2</sub>S levels in saliva samples from college students during exam periods to determine relationships between academic stress and salivary H<sub>2</sub>S over time.<sup>84</sup> Our studies revealed an increase in H<sub>2</sub>S levels over periods of sustained stress and established a correlation of this increase with NO levels, experience of stress, and negative affect.

## 8. PHOTOACTIVATABLE CHEMILUMINESCENCE

In a newer direction, our laboratory has recently explored photoactivatable chemiluminescence. We designed UVC454 and UVA454 with *ortho*-nitrobenzyl protecting groups that are removed upon ultraviolet irradiation, allowing irreversible photochemical uncaging of the chemiluminescent phenolate even in water.<sup>85</sup> Spiro-CL, on the other hand, interconverts between its stable spiropyran form and the metastable merocyanine form upon UV or visible light irradiation (Figure 14). The metastable open form can undergo CIEEL and emit light, thus representing the first example of photoswitchable chemiluminescence, which could have applications for targeted *in vivo* imaging and photoactivatable volumetric 3D displays.<sup>86,87</sup>

## 9. CONCLUSIONS

In this Account, we have documented our research group's development of chemiluminescent 1,2-dioxetanes as triggerable biological imaging probes, specifically for analyzing oxygen, pH, and RSON species (Table 1). Our work helped establish the feasibility of using spiroadamantane 1,2-dioxetanes *in vivo* and demonstrated their use in investigating biological signaling pathways that involve H<sub>2</sub>S, hypoxia, and peroxyxynitrite. To move toward precise quantification, our group showed the first examples of ratiometric imaging using chemiluminescent 1,2-dioxetanes, including a CRET probe for *in vivo* ratiometric pH imaging. We have also pioneered a new approach for quantitative measurement of reactive species, which we call a kinetics-based approach. Whereas a

ratiometric approach achieves quantification by analyses of equilibrium, a kinetics-based approach achieves quantification by careful analysis of reaction rates and mechanisms to deduce analyte concentrations from signal dynamics. This kinetics-based approach was successfully used to quantify HNO concentrations in real-time and provide a quantitative measure of oxygen-dependent enzyme activity in living cells. Finally, we have executed industrial and clinical collaborations to translate chemiluminescence technologies for point-of-care measurement of H<sub>2</sub>O<sub>2</sub> in the exhaled breath condensate of asthma patients.

We also note the excellent work in this area being performed by other groups and provide a brief comparison to our own work. Sun and co-workers<sup>88</sup> developed an acrylic acid 1,2-dioxetane probe for hypoxia based on a nitroaromatic trigger similar to our HyCL series. The acrylic acid group improves aqueous solubility, but HyCL-4-AM features improved cellular uptake. Huang and co-workers<sup>89,90</sup> have developed a series of near-infrared 1,2-dioxetane probes using a formyl ester trigger for peroxyxynitrite detection. The near-infrared emission can image deeper in tissue and the different trigger is likely to have a disparate selectivity from the isatin-based PNCL probe. In comparison to the CHS probes series, Simsek Turan and Somzen,<sup>91</sup> and Levinn and Pluth<sup>92</sup> have reported probes for hydrogen sulfide using dinitrophenyl and azide triggers, although these studies were limited to *in vitro* experiments. More recently, Gholap and co-workers<sup>93</sup> reported a series of hydrogen sulfide 1,2-dioxetane probes with various triggers and used these to study hydrogen sulfide production from  $\beta$ -Lactam antibiotic degradation. Amongst these studies, only the CHS series has been used for *in vivo* imaging of hydrogen sulfide.

The future is bright and open for further development and applications of chemiluminescent 1,2-dioxetanes. Ultimately, more advanced designs may have potential for clinical translation and real-time monitoring of analytes and clinical parameters. The ability to deliver light to deep tissues using chemiluminescent 1,2-dioxetanes has intriguing potential for photopharmacology, radiation therapy, and photodynamic therapy, and these molecules could also be creatively applied in photocatalysis for unique mechanisms of targeted drug release. While we have focused on cellular, animal, and clinical imaging, optimized chemiluminescent agents could be quickly applied to environmental testing for contaminants in water or air. We have recently disclosed a series of photocaged and photoswitchable 1,2-dioxetanes that enable light-mediated spatiotemporal control of chemiluminescence emission. This offers exciting new opportunities for targeted biological imaging and advanced materials like volumetric 3D chemiluminescent displays and formal energy upconversion photonic materials.

## ACKNOWLEDGMENTS

Research reported in this publication was supported by the National Institute of General Medical Sciences of the National Institutes of Health under Award Number R15GM114792-02 and the National Science Foundation under CHE1653474. The content is solely the responsibility of the authors and does not necessarily represent the official views of the National Institutes of Health.

## Biographies

**Uroob Haris** received her B.A. in Chemistry and B.B.A in Management from Southern Methodist University in 2018. She is currently a Ph.D. student in Prof. Alex Lippert's group. Her research interests involve light-driven chemistry, including luminescence imaging and systems for light-based lithography.

**Husain N. Kagalwala** obtained his B.S. in Chemistry (2006) and M.S. in Inorganic Chemistry (2008) from the University of Pune, India. He then pursued graduate studies with Prof. Stefan Bernhard at Carnegie Mellon University, Pittsburgh and received his Ph.D. in 2015. This was followed by postdoctoral research in the laboratories of Prof. Randolph Thummel at University of Houston and Prof. Thomas B. Rauchfuss at University of Illinois, Urbana-Champaign. He is currently working as a research scientist in Prof. Alex Lippert's group, where he is developing near-IR chemiluminescent oxygen sensors.

**Yujin Lisa Kim** is currently a research assistant in Prof. Alex Lippert's research group. She received her B.S. in Biochemistry from Southern Methodist University in 2021. Her research interests include development of assays for quantification of biological molecules in human clinical samples.

**Alexander R. Lippert** received his B.S. degree in 2003 from Caltech, followed by Ph.D. research with Prof. Jeffrey W. Bode where he received his degree from the University of Pennsylvania in 2008. After postdoctoral research with Prof. Christopher J. Chang at the University of California, Berkeley, he started his independent career at Southern Methodist University in 2012 where he is currently an Associate Professor. Prof. Lippert is cofounder and Chief Science Officer (CSO) of BioLum Sciences, LLC, which works toward commercialization of chemiluminescence technologies.

## REFERENCES

- (1). Cao J; Lopez R; Thacker JM; Moon JY; Jiang C; Morris SNS; Bauer JH; Tao P; Mason RP; Lippert AR Chemiluminescent Probes for Imaging H<sub>2</sub>S in Living Animals. *Chem. Sci* 2015, 6, 1979–1985. [PubMed: 25709805] A spiroadamantane 1,2-dioxetane-based chemiluminescent probe is demonstrated to be able to image small molecule analytes in vivo in live mice for the first time.
- (2). Cao J; An W; Reeves AG; Lippert AR A Chemiluminescent Probe for Cellular Peroxynitrite Using a Self-Immolative Oxidative Decarbonylation Reaction. *Chem. Sci* 2018, 9, 2552–2558. [PubMed: 29732134] An enhancer-free 1,2-dioxetane-based chemiluminescent probe is used for direct detection of peroxynitrite generated in cells.
- (3). An W; Ryan LS; Reeves AG; Bruemmer KJ; Mouhaffel M; Gerberich JL; Winters A; Mason RP; Lippert AR A Chemiluminescent Probe for HNO Quantification and Real-time Monitoring in Living Cells. *Angew. Chem., Int. Ed* 2019, 58, 1361–1365. A kinetics-based method is formulated and implemented for quantification of small molecules based on kinetic response of a triggerable chemiluminescent probe.
- (4). Ryan LS; Gerberich J; Haris U; Nguyen D; Mason RP; Lippert AR Ratiometric pH Imaging Using a 1,2-Dioxetane Chemiluminescence Resonance Energy Transfer Sensor in Live Animals. *ACS Sens.* 2020, 5, 2925–2932. [PubMed: 32829636] A single-molecule energy transfer chemiluminescent probe is investigated and used for ratiometric quantification of pH with demonstrated viability in living mice.

- (5). Bruemmer KJ; Crossley SWM; Chang CJ Activity-Based Sensing: A Synthetic Methods Approach for Selective Molecular Imaging and Beyond. *Angew. Chem., Int. Ed* 2020, 59, 13734–13762.
- (6). Xie D; Yu M; Kadakia RT; Que EL <sup>19</sup>F Magnetic Resonance Activity-Based Sensing Using Paramagnetic Metals. *Acc. Chem. Res* 2020, 53, 2–10. [PubMed: 31809009]
- (7). Chan J; Dodani SC; Chang CJ Reaction-based small-molecule fluorescent probes for chemoselective bioimaging. *Nat. Chem* 2012, 4, 973–984. [PubMed: 23174976]
- (8). Carter KP; Young AM; Palmer AE Fluorescent Sensors for Measuring Metal Ions in Living Systems. *Chem. Rev* 2014, 114, 4564–4601. [PubMed: 24588137]
- (9). Gnaim S; Shabat D Activity-Based Optical Sensing Enabled by Self-Immolative Scaffolds: Monitoring of Release Events by Fluorescence and Chemiluminescence Output. *Acc. Chem. Res* 2019, 52, 2806–2817. [PubMed: 31483607]
- (10). Grynkiewicz G; Poenie M; Tsien RY A New Generation of Ca<sup>2+</sup> Indicators with Greatly Improved Fluorescence Properties. *J. Biol. Chem* 1985, 260, 3440–3450. [PubMed: 3838314]
- (11). Nolan EM; Lippard SJ Small-Molecule Fluorescent Sensors for Investigating Zinc Metalloneurochemistry. *Acc. Chem. Res* 2009, 42, 193–203. [PubMed: 18989940]
- (12). Que EL; Bleher R; Duncan FE; Kong BY; Gleber SC; Vogt S; Chen S; Garwin SA; Bayer AR; Dravid VP; Woodruff TK; O'Halloran TV Quantitative Mapping of Zinc Fluxes in the Mammalian Egg Reveals the Origin of Fertilization-Induced Zinc Sparks. *Nat. Chem* 2015, 7, 130–139. [PubMed: 25615666]
- (13). Lazarou TS; Buccella D Advances in Imaging of Understudied Ions in Signaling: A Focus on Magnesium. *Curr. Opin. Chem. Biol* 2020, 57, 27–33. [PubMed: 32408221]
- (14). Wang Z; Detomasi TC; Chang CJ A Dual-Fluorophore Sensor Approach for Ratiometric Fluorescence Imaging of Potassium in Living Cells. *Chem. Sci* 2021, 12, 1720–1729.
- (15). Cotruvo JA Jr.; Aron AT; Ramos-Torres KM; Chang CJ Synthetic Fluorescent Probes for Studying Copper in Biological Systems. *Chem. Soc. Rev* 2015, 44, 4400–4414. [PubMed: 25692243]
- (16). Aron AT; Reeves AG; Chang CJ Activity-based Sensing Fluorescent Probes for Iron in Biological Systems. *Curr. Opin. Chem. Biol* 2018, 43, 113–118. [PubMed: 29306820]
- (17). Han J; Burgess K Fluorescent Indicators for Intracellular pH. *Chem. Rev* 2010, 110, 2709–2728. [PubMed: 19831417]
- (18). Tutol JN; Kam HC; Dodani SC Identification of mNeonGreen as a pH-dependent, Turn-On Fluorescent Protein Sensor for Chloride. *ChemBioChem* 2019, 20, 1759–1765. [PubMed: 30843313]
- (19). Prakash V; Saha S; Chakraborty K; Krishnan Y Rational Design of a Quantitative, pH-insensitive, Nucleic Acid Based Fluorescent Chloride Reporter. *Chem. Sci* 2016, 7, 1946–1953. [PubMed: 30050672]
- (20). Liu P; Miller EW Electrophysiology, Unplugged: Imaging Membrane Potential with Fluorescent Indicators. *Acc. Chem. Res* 2020, 53, 11–19. [PubMed: 31834772]
- (21). Lippert AR Designing Reaction-Based Fluorescent Probes for Selective Hydrogen Sulfide Detection. *J. Inorg. Biochem* 2014, 133, 136–142. [PubMed: 24239492]
- (22). Bezner BJ; Ryan LS; Lippert AR Reaction-Based Luminescent Probes for Reactive Sulfur, Oxygen, and Nitrogen Species: Analytical Techniques and Recent Progress. *Anal. Chem* 2020, 92, 309–326. [PubMed: 31679337]
- (23). Cortese-Krott MM; Koning A; Kuhnle GGC; Nagy P; Bianco CL; Pasch A; Wink DA; Fukuto JM; Jackson AA; van Goor H; Olson KR; Feelisch M The Reactive Species Interactome: Evolutionary Emergence, Biological Significance, and Opportunities for Redox Metabolomics and Personalized Medicine. *Antioxid. Redox Signaling* 2017, 27, 684–712.
- (24). Kaur A; New EJ Bioinspired Small-Molecule Tools for the Imaging of Redox Biology. *Acc. Chem. Res* 2019, 52, 623–632. [PubMed: 30747522]
- (25). Lippert AR; Van de Bittner GC; Chang CJ Boronate Oxidation as a Bioorthogonal Reaction Approach for Studying the Chemistry of Hydrogen Peroxide in Living Systems. *Acc. Chem. Res* 2011, 44, 793–804. [PubMed: 21834525]

- (26). Bai X; Ng KKH; Hu JJ; Ye S; Yang D Small-Molecule-Based Fluorescent Sensors for Selective Detection of Reactive Oxygen Species in Biological Systems. *Annu. Rev. Biochem* 2019, 88, 605–633. [PubMed: 31018111]
- (27). Kojima H; Urano Y; Kikuchi K; Higuchi T; Hirata Y; Nagano T Fluorescent Indicators for Imaging Nitric Oxide Production. *Angew. Chem., Int. Ed* 1999, 38, 3209–3212.
- (28). Lau N; Pluth MD Reactive Sulfur Species (RSS): Persulfides, Polysulfides, Potential, and Problems. *Curr. Opin. Chem. Biol* 2019, 49, 1–8. [PubMed: 30243097]
- (29). Lin VS; Chen W; Xian M; Chang CJ Chemical Probes for Molecular Imaging and Detection of Hydrogen Sulfide and Reactive Sulfur Species in Biological Systems. *Chem. Soc. Rev* 2015, 44, 4596–4618. [PubMed: 25474627]
- (30). Liu H; Radford MN; Yang CT; Chen W; Xian M Inorganic hydrogen polysulfides: chemistry, chemical biology and detection. *Br. J. Pharmacol* 2019, 176, 616–627. [PubMed: 29669174]
- (31). Bruemmer KJ; Brewer TF; Chang CJ Fluorescent Probes for Imaging Formaldehyde in Biological Systems. *Curr. Opin. Chem. Biol* 2017, 39, 17–23. [PubMed: 28527906]
- (32). Ohata J; Bruemmer KJ; Chang CJ Activity-Based Sensing Methods for Monitoring the Reactive Carbon Species Carbon Monoxide and Formaldehyde in Living Systems. *Acc. Chem. Res* 2019, 52, 2841–2848. [PubMed: 31487154]
- (33). Krohn KA; Link JM; Mason RP Molecular Imaging of Hypoxia. *J. Nucl. Med* 2008, 49, 129S–148S. [PubMed: 18523070]
- (34). Kolanowski JL; Liu F; New EJ Fluorescent Probes for the Simultaneous Detection of Multiple Analytes in Biology. *Chem. Soc. Rev* 2018, 47, 195–208. [PubMed: 29119192]
- (35). Wu L; Sedgwick AC; Sun X; Bull SD; He XP; James TD Reaction-Based Fluorescent Probes for the Detection and Imaging of Reactive Oxygen, Nitrogen, and Sulfur Species. *Acc. Chem. Res* 2019, 52, 2582–2597. [PubMed: 31460742]
- (36). Liu L; Mason RP Imaging beta-galactosidase Activity in Human Tumor Xenografts and Transgenic Mice Using a Chemiluminescent Substrate. *PLoS One* 2010, 5, e12024. [PubMed: 20700459]
- (37). Green O; Eilon T; Hananya N; Gutkin S; Bauer CR; Shabat D Opening a Gateway for Chemiluminescence Cell Imaging: Distinctive Methodology for Design of Bright Chemiluminescent Dioxetane Probes. *ACS Cent. Sci* 2017, 3, 349–358. [PubMed: 28470053]
- (38). Lippert AR Unlocking the Potential of Chemiluminescence Imaging. *ACS Cent. Sci* 2017, 3, 269–271. [PubMed: 28470041]
- (39). Schaap AP; Handley RS; Giri BP Chemical and Enzymatic Triggering of 1,2-Dioxetanes. 1: Aryl Esterase-catalyzed Chemiluminescence from a Naphthyl Acetate-Substituted Dioxetane. *Tetrahedron Lett.* 1987, 28, 935–938.
- (40). Schaap AP; Chen TS; Handley RS; DeSilva R; Giri BP Chemical and Enzymatic Triggering of 1,2-Dioxetanes. 2: Fluoride-induced Chemiluminescence from *tert*-Butyldimethylsilyloxy-substituted Dioxetanes. *Tetrahedron Lett.* 1987, 28, 1155–1158.
- (41). Schaap AP; Sandison MD; Handley RS Chemical and Enzymatic Triggering of 1,2-Dioxetanes. 3: Alkaline Phosphatase-catalyzed Chemiluminescence from an Aryl Phosphate-substituted Dioxetane. *Tetrahedron Lett.* 1987, 28, 1159–1162.
- (42). Vacher M; Fdez. Galván I; Ding BW; Schramm S; Berraud-Pache R; Naumov P; Ferré N; Liu Y-J; Navizet I; Roca-Sanjuán D; Baader WJ; Lindh R Chemi- and Bioluminescence of Cyclic Peroxides. *Chem. Rev* 2018, 118, 6927–6974. [PubMed: 29493234]
- (43). Adam W; Bronstein I; Trofimov AV; Vasil'ev RF Solvent-Cage Effect (Viscosity Dependence) as a Diagnostic Probe for the Mechanism of the Intramolecular Chemically Initiated Electron-Exchange Luminescence (CIEEL) Triggered from a Spiroadmantyl-Substituted Dioxetane. *J. Am. Chem. Soc* 1999, 121, 958–961.
- (44). Augusto FA; De Souza GA; de Souza Júnior SP; Khalid M; Baader WJ Efficiency of Electron Transfer Initiated Chemiluminescence. *Photochem. Photobiol* 2013, 89, 1299–1317. [PubMed: 23711099]
- (45). Hoshiya N; Fukuda N; Maeda H; Watanabe N; Matsumoto M Synthesis and Fluoride-induced Chemiluminescent Decomposition of Bicyclic Dioxetanes Substituted with a 2-Hydroxynaphthyl Group. *Tetrahedron* 2006, 62, 5808–5820.

- (46). Yue L; Liu YJ Mechanism of AMPPD Chemiluminescence in a Different Voice. *J. Chem. Theory Comput* 2013, 9, 2300–2312. [PubMed: 26583723]
- (47). Hananya N; Shabat D Recent Advances and Challenges in Luminescent Imaging: Bright Outlook for Chemiluminescence of Dioxetanes in Water. *ACS Cent. Sci* 2019, 5, 949–959. [PubMed: 31263754]
- (48). Gnaïm S; Green O; Shabat D The Emergence of Aqueous Chemiluminescence: New Promising Class of Phenoxy 1,2-Dioxetane Luminophores. *Chem. Commun* 2018, 54, 2073–2085.
- (49). Hananya N; Shabat D A Glowing Trajectory between Bio- and Chemiluminescence: From Luciferin-Based Probes to Triggerable Dioxetanes. *Angew. Chem., Int. Ed* 2017, 56, 16454–16463.
- (50). Lippert AR; New EJ; Chang CJ Reaction-Based Fluorescent Probes for the Selective Imaging of Hydrogen Sulfide in Living Cells. *J. Am. Chem. Soc* 2011, 133, 10078–10080. [PubMed: 21671682]
- (51). Yang G; Wu L; Jiang B; Yang W; Qi J; Cao K; Meng Q; Mustafa AK; Mu W; Zhang S; Snyder SH; Wang R H<sub>2</sub>S as a Physiologic Vasorelaxant: Hypertension in Mice with Deletion of Cystathionine  $\gamma$ -Lyase. *Science* 2008, 322, 587–590. [PubMed: 18948540]
- (52). Peng YJ; Nanduri J; Raghuraman G; Souvannakitti D; Gadalla MM; Kumar GK; Snyder SH; Prabhakar NR H<sub>2</sub>S Mediates O<sub>2</sub> Sensing in the Carotid Body. *Proc. Natl. Acad. Sci. U. S. A* 2010, 107, 10719–10724. [PubMed: 20556885]
- (53). Papapetropoulos A; Pyriochou A; Altaany Z; Yang G; Marazioti A; Zhou Z; Jeschke MG; Branski LK; Herndon DN; Wang R; Szabó C Hydrogen Sulfide is an Endogenous Stimulator of Angiogenesis. *Proc. Natl. Acad. Sci. U. S. A* 2009, 106, 21972–21977. [PubMed: 19955410]
- (54). Paul BD; Sbodio JI; Xu R; Vandiver MS; Cha JY; Snowman AM; Snyder SH Cystathionine  $\gamma$ -Lyase Deficiency Mediates Neurodegeneration in Huntington's Disease. *Nature* 2014, 509, 96–100. [PubMed: 24670645]
- (55). Lin VS; Lippert AR; Chang CJ Cell-trappable Fluorescent Probes for Endogenous Hydrogen Sulfide Signaling and Imaging H<sub>2</sub>O<sub>2</sub>-dependent H<sub>2</sub>S Production. *Proc. Natl. Acad. Sci. U. S. A* 2013, 110, 7131–7135. [PubMed: 23589874]
- (56). Ju L; Lippert AR; Bode JW Stereoretentive Synthesis and Chemoselective Amide-Forming Ligations of C-Terminal Peptide  $\alpha$ -Ketoacids. *J. Am. Chem. Soc* 2008, 130, 4253–4255. [PubMed: 18335941]
- (57). Reeves AG; Subbarao M; Lippert AR Imaging Acetaldehyde Formation During Ethanol Metabolism in Living Cells Using a Hydrazine Naphthalimide Fluorescent Probe. *Anal. Methods* 2017, 9, 3418–3421. [PubMed: 29109756]
- (58). Pacher P; Beckman JS; Liaudet L Nitric Oxide and Peroxynitrite in Health and Disease. *Physiol. Rev* 2007, 87, 315–424. [PubMed: 17237348]
- (59). Bruemmer KJ; Merrikhihaghi S; Lollar CT; Morris SNS; Bauer JH; Lippert AR <sup>19</sup>F Magnetic Resonance Probes for Detecting Peroxynitrite in Living Cells Using an Oxidative Decarbonylation Reaction. *Chem. Commun* 2014, 50, 12311–12314.
- (60). Cao J; Campbell J; Liu L; Mason RP; Lippert AR In Vivo Chemiluminescent Imaging Agents for Nitroreductase and Tissue Oxygenation. *Anal. Chem* 2016, 88, 4995–5002. [PubMed: 27054463]
- (61). Huang X; Song J; Yung BC; Huang X; Xiong Y; Chen X Ratiometric Optical Nanoprobes Enable Accurate Molecular Detection and Imaging. *Chem. Soc. Rev* 2018, 47, 2873–2920. [PubMed: 29568836]
- (62). Aoi W; Marunaka Y Importance of pH Homeostasis in Metabolic Health and Diseases: Crucial Role of Membrane Proton Transport. *BioMed Res. Int* 2014, 2014, 598986. [PubMed: 25302301]
- (63). Boedtker E; Pedersen SF The Acidic Tumor Microenvironment as a Driver of Cancer. *Annu. Rev. Physiol* 2020, 82, 103–126. [PubMed: 31730395]
- (64). Ma T; Hou Y; Zeng J; Liu C; Zhang P; Jing L; Shanguan D; Gao M Dual-Ratiometric Target-Triggered Fluorescent Probe for Simultaneous Quantitative Visualization of Tumor Microenvironment Protease Activity and pH *in Vivo*. *J. Am. Chem. Soc* 2018, 140, 211–218. [PubMed: 29237264]

- (65). Pratiwi FW; Hsia CH; Kuo CW; Yang SM; Hwu YK; Chen P Construction of Single Fluorophore Ratiometric pH Sensors Using Dual-Emission Mn<sup>2+</sup>-Doped Quantum Dots. *Biosens. Bioelectron* 2016, 84, 133–140. [PubMed: 26852157]
- (66). Richardson DS; Gregor C; Winter FR; Urban NT; Sahl SJ; Willig KI; Hell SW SRpHi Ratiometric pH Biosensors for Super-Resolution Microscopy. *Nat. Commun* 2017, 8, 577. [PubMed: 28924139]
- (67). Hanson GT; McAnaney TB; Park ES; Rendell MEP; Yarbrough DK; Chu S; Xi L; Boxer SG; Montrose MH; Remington SJ Green Fluorescent Protein Variants as Ratiometric Dual Emission pH Sensors. 1. Structural Characterization and Preliminary Application. *Biochemistry* 2002, 41, 15477–15488. [PubMed: 12501176]
- (68). An W; Mason RP; Lippert AR Energy Transfer Chemiluminescence for Ratiometric pH Imaging. *Org. Biomol. Chem* 2018, 16, 4176–4182. [PubMed: 29786719]
- (69). Zhang G; Jacquemin D; Buccella D Tuning the Spectroscopic Properties of Ratiometric Fluorescent Metal Indicators: Experimental and Computational Studies on Mag-fura-2 and Analogues. *J. Phys. Chem. B* 2017, 121, 696–705. [PubMed: 28052199]
- (70). Egawa T; Hanaoka K; Koide Y; Ujita S; Takahashi N; Ikegaya Y; Matsuki N; Terai T; Ueno T; Komatsu T; Nagano T Development of a Far-Red to Near-Infrared Fluorescence Probe for Calcium Ion and its Application to Multicolor Neuronal Imaging. *J. Am. Chem. Soc* 2011, 133, 14157–14159. [PubMed: 21827169]
- (71). Chen J; Jiang X; Zhang C; MacKenzie KR; Stossi F; Palzkill T; Wang MC; Wang J Reversible Reaction-Based Fluorescent Probe for Real-Time Imaging of Glutathione Dynamics in Mitochondria. *ACS Sens* 2017, 2, 1257–1261. [PubMed: 28809477]
- (72). Jiang X; Yu Y; Chen J; Zhao M; Chen H; Song X; Matzuk AJ; Carroll SL; Tan X; Sizovs A; Cheng N; Wang MC; Wang J Quantitative Imaging of Glutathione in Live Cells Using a Reversible Reaction-Based Ratiometric Fluorescent Probe. *ACS Chem. Biol* 2015, 10, 864–874. [PubMed: 25531746]
- (73). Myochin T; Kiyose K; Hanaoka K; Kojima H; Terai T; Nagano T Rational Design of Ratiometric Near-Infrared Fluorescent pH Probes with Various pK<sub>a</sub> Values, Based on Aminocyanine. *J. Am. Chem. Soc* 2011, 133, 3401–3409. [PubMed: 21341656]
- (74). Suarez SA; Bikiel DA; Wetzler DE; Marti MA; Doctorovich F Time-Resolved Electrochemical Quantification of Azanone (HNO) at Low Nanomolar Level. *Anal. Chem* 2013, 85, 10262–10269. [PubMed: 23952708]
- (75). Cowart D; Venuti R; Guptill J; Noveck R; Foo S A Phase 1 Study of the Safety and Pharmacokinetics of the Intravenous Nitroxyl Prodrug, CXL-1427. *J. Am. Coll. Cardiol* 2015, 65, A876.
- (76). Ryan LS; Gerberich J; Cao J; An W; Jenkins BA; Mason RP; Lippert AR Kinetics-Based Measurement of Hypoxia in Living Cells and Animals Using an Acetoxymethyl Ester Chemiluminescent Probe. *ACS Sens.* 2019, 4, 1391–1398. [PubMed: 31002225]
- (77). Wortel RC; Mizrahi A; Li H; Markovsky E; Enyedi B; Jacobi J; Brodsky O; Cao J; Lippert AR; Incrocci L; Mulhall JP; Haimovitz-Friedman A Sildenafil Protects Endothelial Cells from Radiation-Induced Oxidative Stress. *J. Sex. Med* 2019, 16, 1721–1733. [PubMed: 31585804]
- (78). Zelefsky MJ; Cowen D; Fuks Z; Shike M; Burman C; Jackson A; Venkatramen ES; Leibel SA Long Term Tolerance of High Dose Three-dimensional Conformal Radiotherapy in Patients with Localized Prostate Carcinoma. *Cancer* 1999, 85, 2460–2468. [PubMed: 10357419]
- (79). Zelefsky MJ; Shasha D; Branco RD; Kollmeier M; Baser RE; Pei X; Ennis R; Stock R; Bar-Chama N; Mulhall JP Prophylactic Sildenafil Citrate Improves Select Aspects of Sexual Function in Men Treated with Radiotherapy for Prostate Cancer. *J. Urol* 2014, 192, 868–874. [PubMed: 24603102]
- (80). Gebaska MA; Stevenson BK; Hemnes AR; Bivalacqua TJ; Haile A; Hesketh GG; Murray CI; Zaiman AL; Halushka MK; Krongkaew N; Strong TD; Cooke CA; El-Haddad H; Tuder RM; Berkowitz DE; Champion HC Phosphodiesterase-5A (PDE5A) is Localized to the Endothelial Caveolae and Modulates NOS3 Activity. *Cardiovasc. Res* 2011, 90, 353–363. [PubMed: 21421555]

- (81). Jones KA; Kentala K; Beck MW; An W; Lippert AR; Lewis JC; Dickinson BC Development of a Split Esterase for Protein-Protein Interaction-Dependent Small-Molecule Activation. *ACS Cent. Sci* 2019, 5, 1768–1776. [PubMed: 31807678]
- (82). Quimbar ME; Krenek KM; Lippert AR A Chemiluminescent Platform for Smartphone Monitoring of H<sub>2</sub>O<sub>2</sub> in Human Exhaled Breath Condensates. *Methods* 2016, 109, 123–130. [PubMed: 27233749]
- (83). Quimbar ME; Davis SQ; Al-Farra ST; Hayes A; Jovic V; Masuda M; Lippert AR Chemiluminescent Measurement of Hydrogen Peroxide in Exhaled Breath Condensate of Healthy and Asthmatic Adults. *Anal. Chem* 2020, 92, 14594–14600. [PubMed: 33064450]
- (84). Kroll JL; Werchan CA; Reeves AG; Bruemmer KJ; Lippert AR; Ritz T Sensitivity of Salivary Hydrogen Sulfide to Psychological Stress and its Association with Exhaled Nitric Oxide and Affect. *Physiol. Behav* 2017, 179, 99–104. [PubMed: 28527680]
- (85). Ryan LS; Nakatsuka A; Lippert AR Photoactivatable 1,2 Dioxetane Chemiluminophores. *Results in Chemistry* 2021, 3, 100106.
- (86). Patel SK; Cao J; Lippert AR A Volumetric Three-Dimensional Digital Light Photoactivatable Dye Display. *Nat. Commun* 2017, 8, 15239. [PubMed: 28695887]
- (87). Li B; Haris U; Aljowni M; Nakatsuka A; Patel SK; Lippert AR Tuning the Photophysical Properties of Spirolactam Rhodamine Photoswitches. *Isr. J. Chem* 2021, 61, 244–252.
- (88). Sun J; Hu Z; Wang R; Zhang S; Zhang X A Highly Sensitive Chemiluminescent Probe for Detecting Nitroreductase and Imaging in Living Animals. *Anal. Chem* 2019, 91, 1384–1390. [PubMed: 30582678]
- (89). Huang J; Huang J; Cheng P; Jiang Y; Pu K Near-Infrared Chemiluminescent Reporters for In Vivo Imaging of Reactive Oxygen and Nitrogen Species in Kidneys. *Adv. Funct. Mater* 2020, 30, 2003628.
- (90). Huang J; Jiang Y; Li J; Huang J; Pu K Molecular Chemiluminescent Probes with a Very Long Near-Infrared Emission Wavelength for in Vivo Imaging. *Angew. Chem* 2021, 133, 4045–4049.
- (91). Simsek Turan I; Sozmen F A Chromogenic Dioxetane Chemosensor for Hydrogen Sulfide and pH Dependent Off–On Chemiluminescence Property. *Sens. Actuators, B* 2014, 201, 13–18.
- (92). Levinn CM; Pluth MD Direct Comparison of Triggering Motifs on Chemiluminescent Probes for Hydrogen Sulfide Detection in Water. *Sens. Actuators, B* 2021, 329, 129235.
- (93). Gholap SP; Yao C; Green O; Babjak M; Jakubec P; Malatinsky T; Ihssen J; Wick L; Spitz U; Shabat D Chemiluminescence Detection of Hydrogen Sulfide Release by  $\beta$ -Lactamase-Catalyzed  $\beta$ -Lactam Biodegradation: Unprecedented Pathway for Monitoring  $\beta$ -Lactam Antibiotic Bacterial Resistance. *Bioconjugate Chem.* 2021, 32, 991.



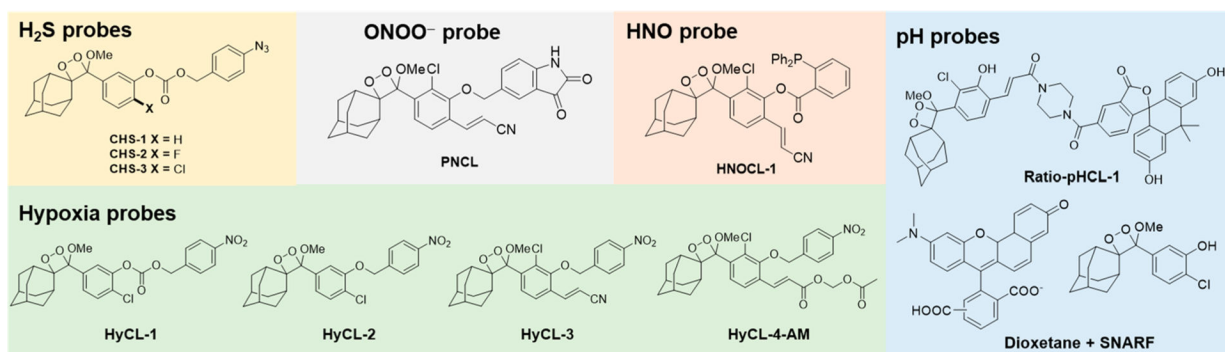


**Figure 1.**  
 Chemiluminescent 1,2-dioxetane probes developed by our laboratory for the detection of biological analytes.

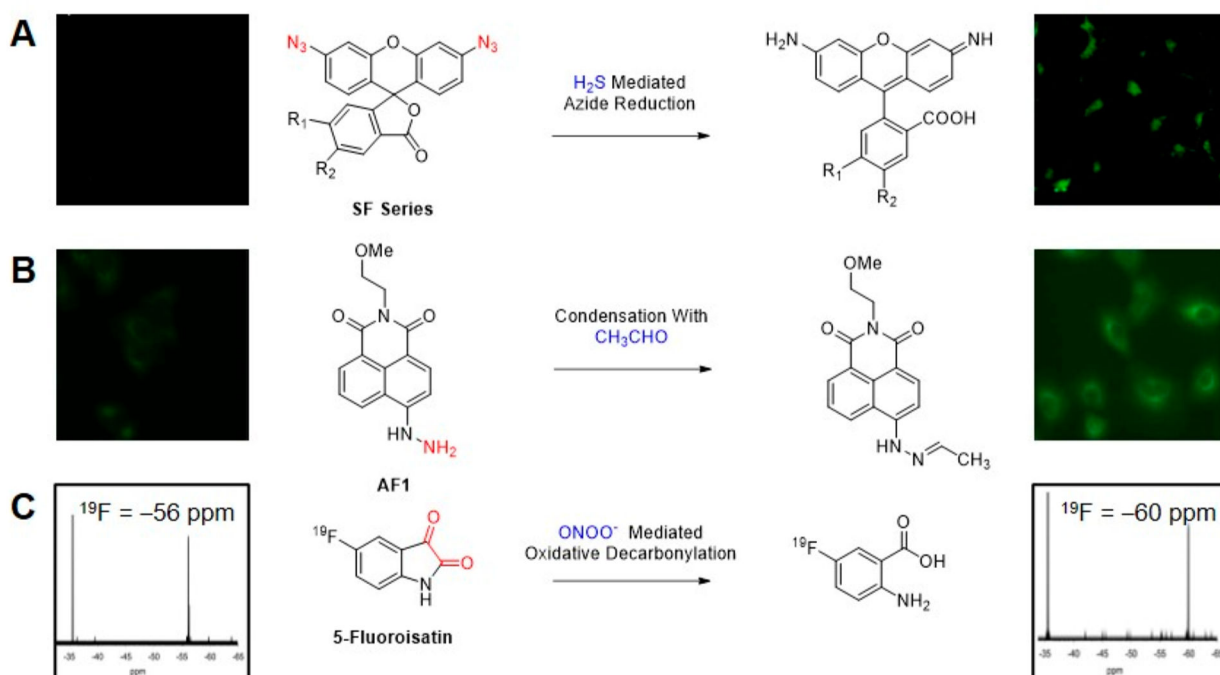


**Figure 2.** Reaction-based fluorescence and magnetic resonance probes for reactive species. (A) SF Series of probes for fluorescence imaging of  $\text{H}_2\text{S}$ . Adapted with permission from ref 50. Copyright 2013 American Chemical Society. (B) AF1 for fluorescence imaging of acetaldehyde. Adapted with permission from ref 57. Copyright 2017 The Royal Society of Chemistry. (C) 5-Fluoroisatin for  $^{19}\text{F}$  NMR detection of  $\text{ONOO}^-$ . Adapted with permission from ref 59. Copyright 2014 The Royal Society of Chemistry.

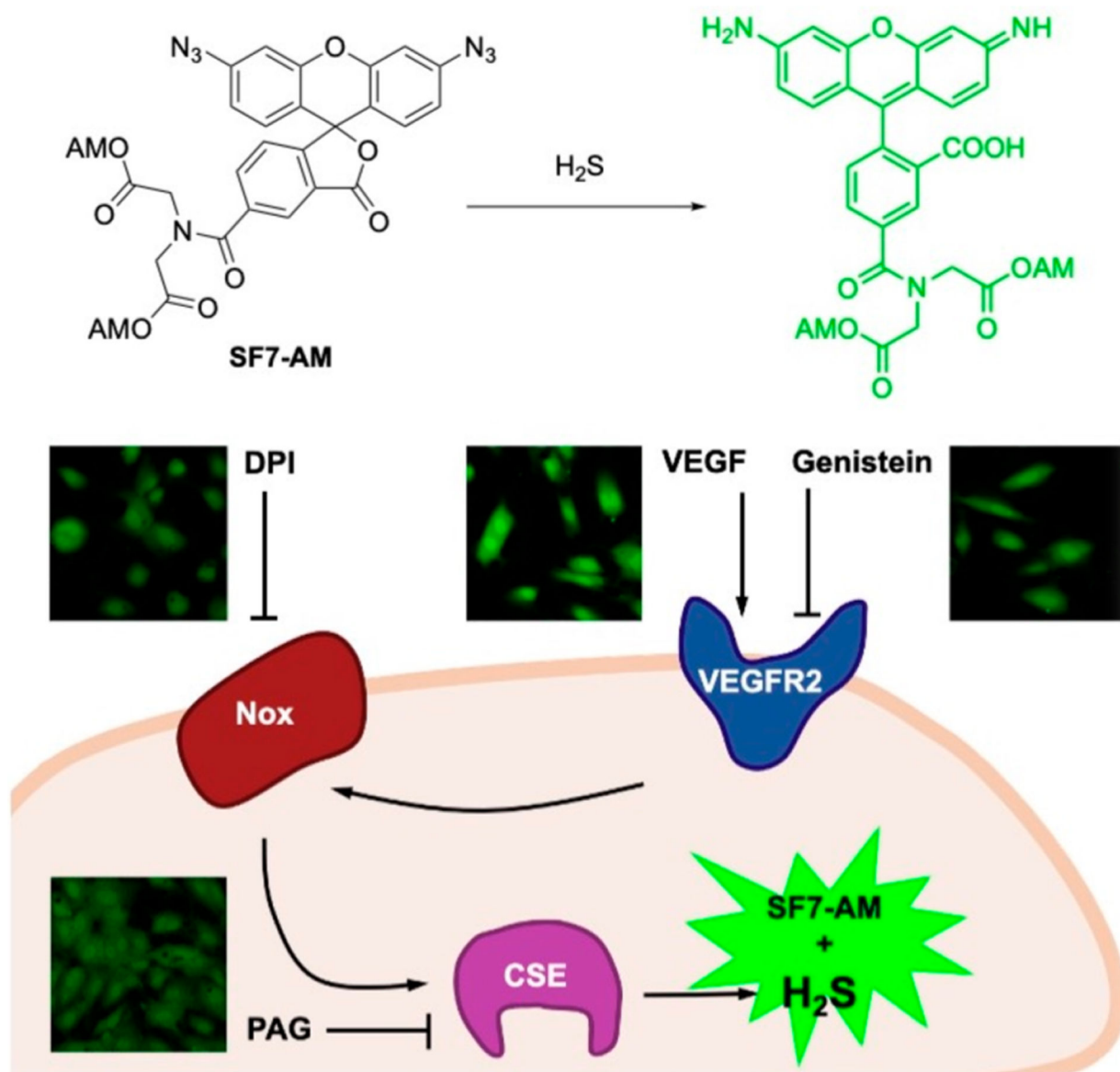


**Figure 3.** SF7-AM was used to monitor VEGF-induced  $H_2S$  production in HUVEC cells. Adapted with permission from ref 55. Copyright 2011 United States National Academy of Sciences.

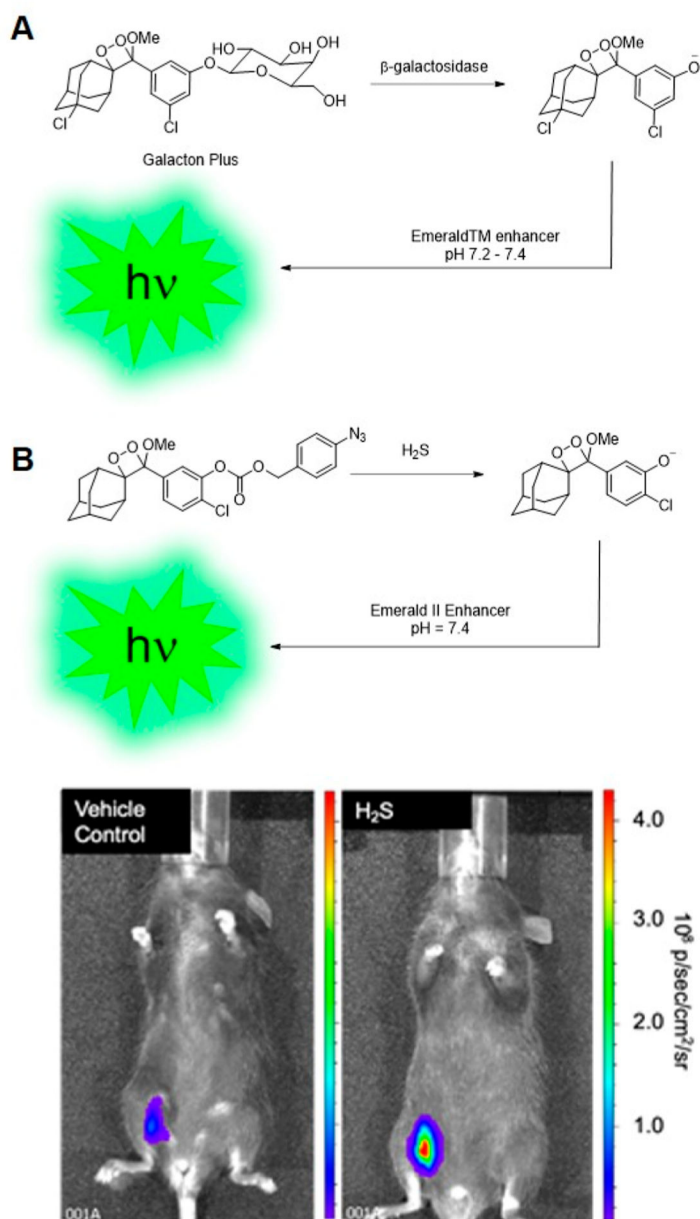


**Figure 4.** Probes demonstrated as *in vivo* chemiluminescence imaging agents. (A) Commercially available Galacto-Light Plus chemiluminescence assay adapted for imaging  $\beta$ -galactosidase enzymatic activity in mice. (B) Chemiluminescence  $H_2S$  imaging in live mice using CHS-3. Adapted with permission from ref 1. Copyright 2015 The Royal Society of Chemistry.

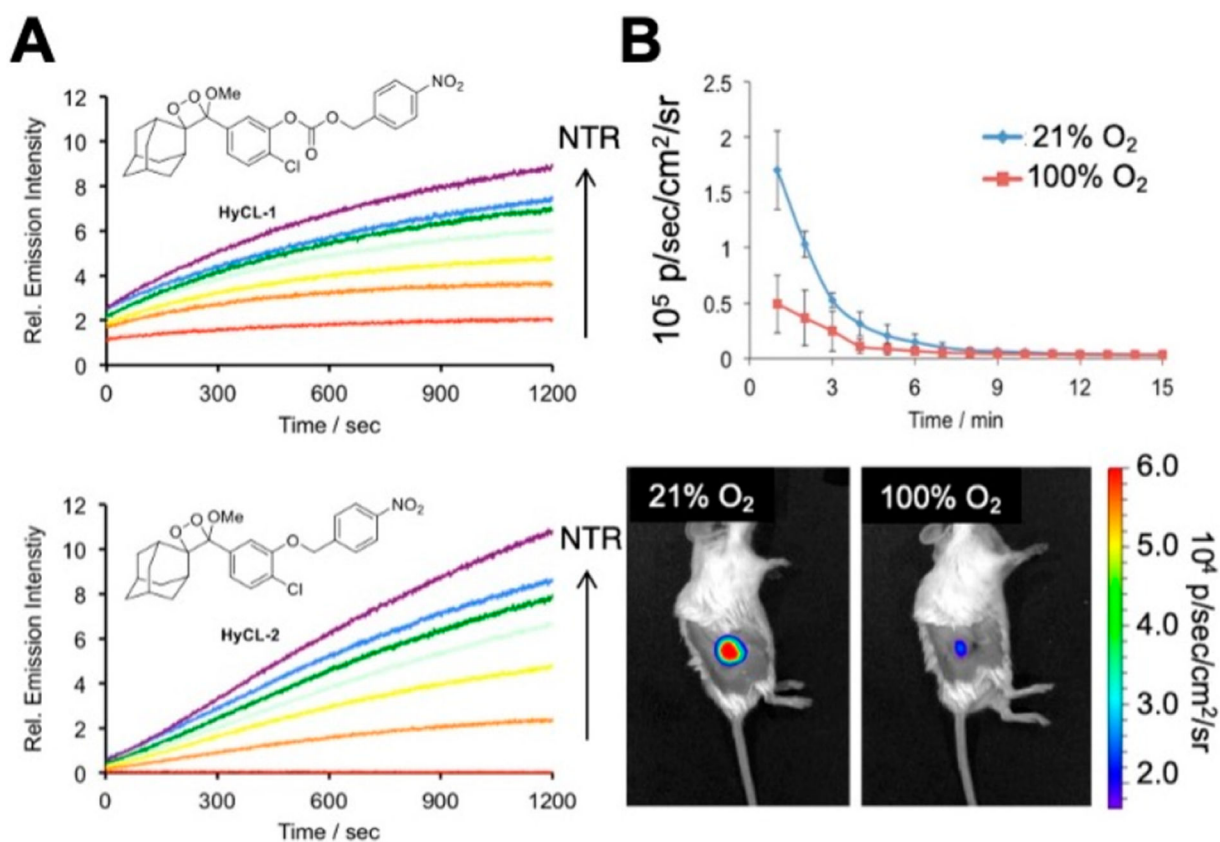


**Figure 5.**

Hypoxia imaging in tumor xenograft models with HyCL-2. (A) Comparison of the carbonate-linked HyCL-1 to the ether linked HyCL-2 reveals significant reduction in background signal. (B) Imaging hypoxia in tumor xenograft models using HyCL-2 while mice breathed 21% or 100% oxygen. Adapted with permission from ref 60. Copyright 2016 American Chemical Society.

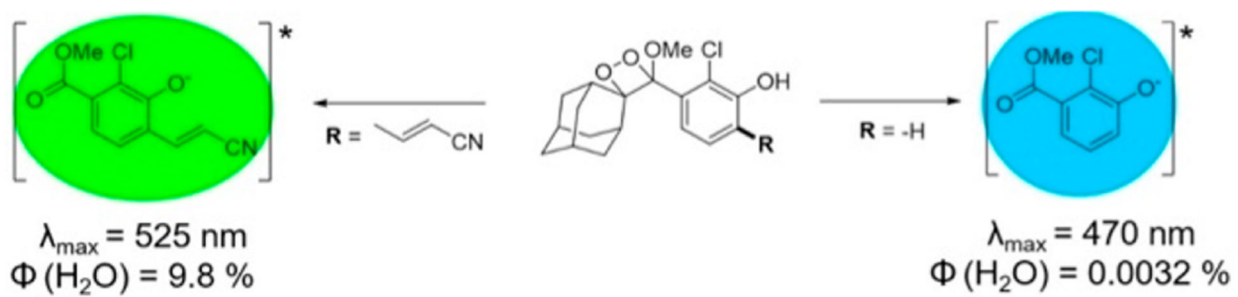


**Figure 6.** Substitution of an acrylonitrile group dramatically increases the chemiluminescence quantum yield of spiroadamantane 1,2-dioxetanes.

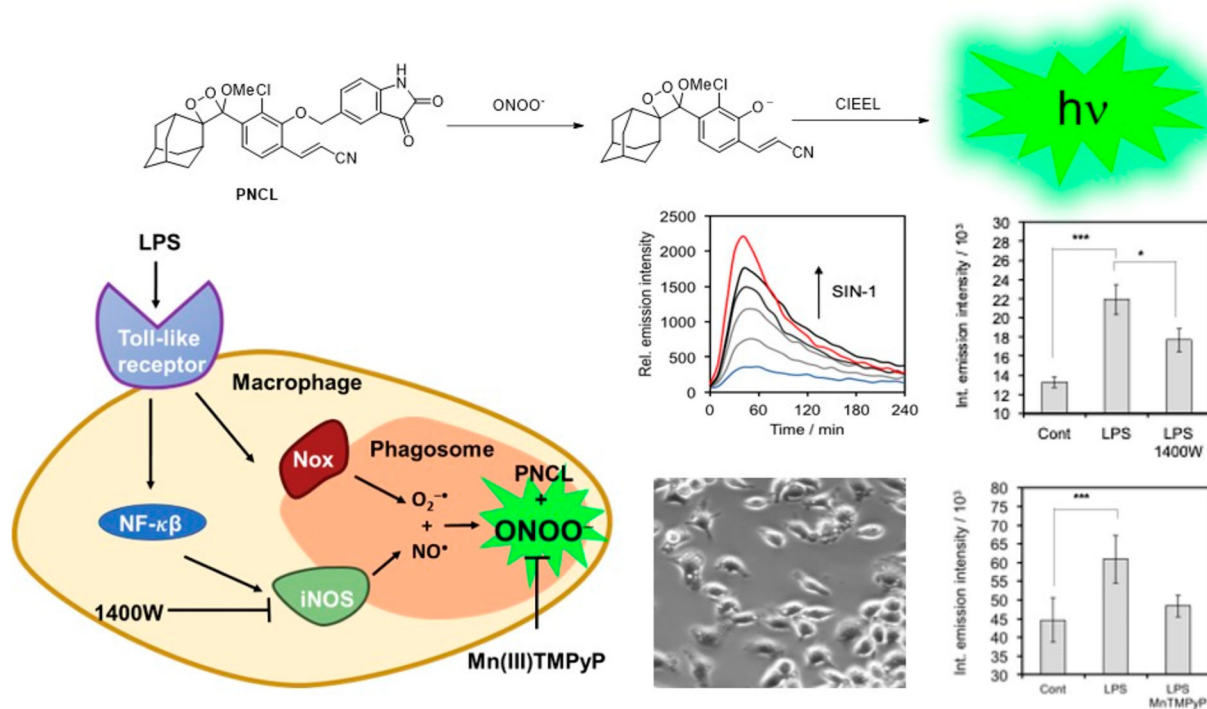


**Figure 7.**

Interrogating cellular immune response with PNCL. Treatment of RAW 264.7 macrophages with lipopolysaccharide (LPS) induces phagosome formation and iNOS-dependent formation of  $\text{ONOO}^-$ . Adapted with permission from ref 2. Copyright 2018 The Royal Society of Chemistry.

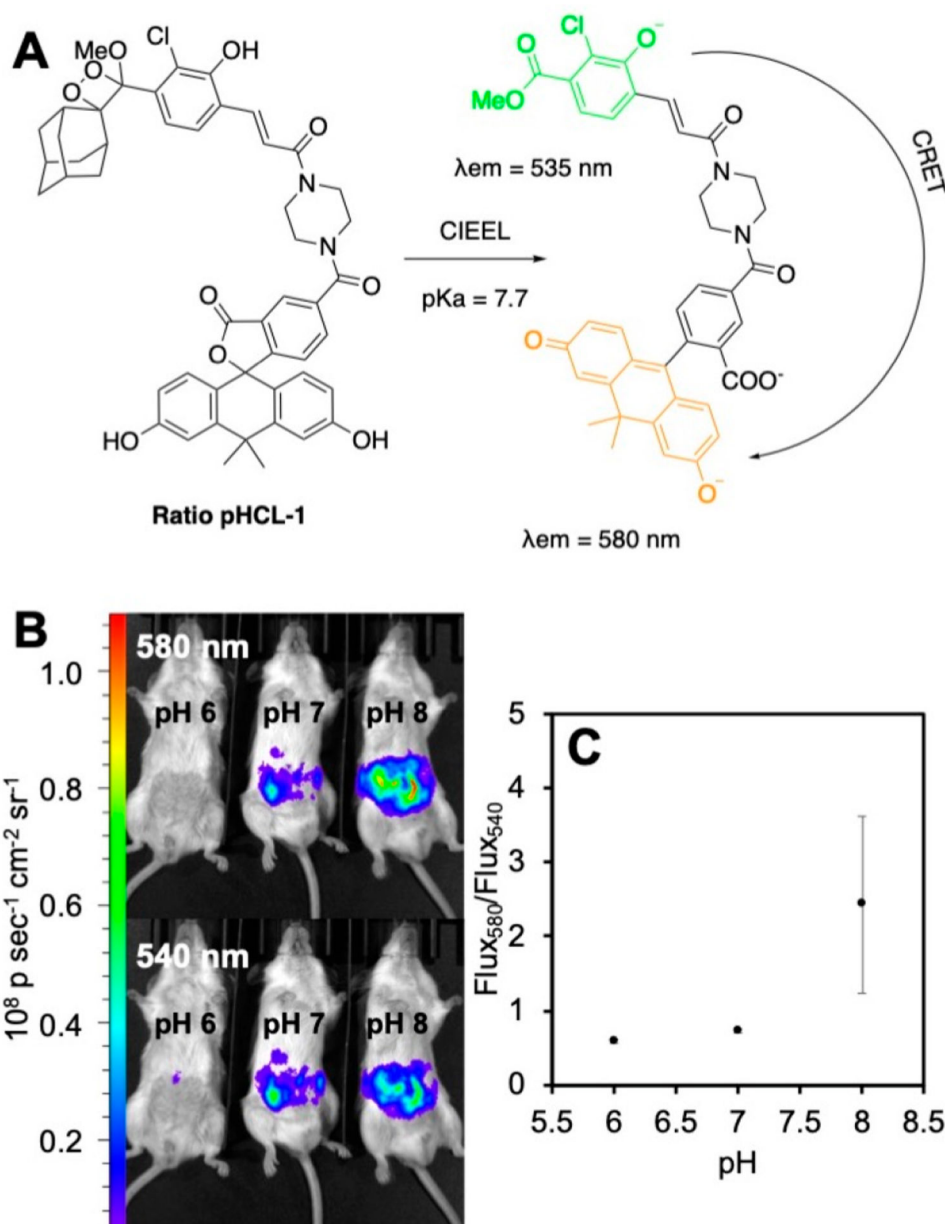
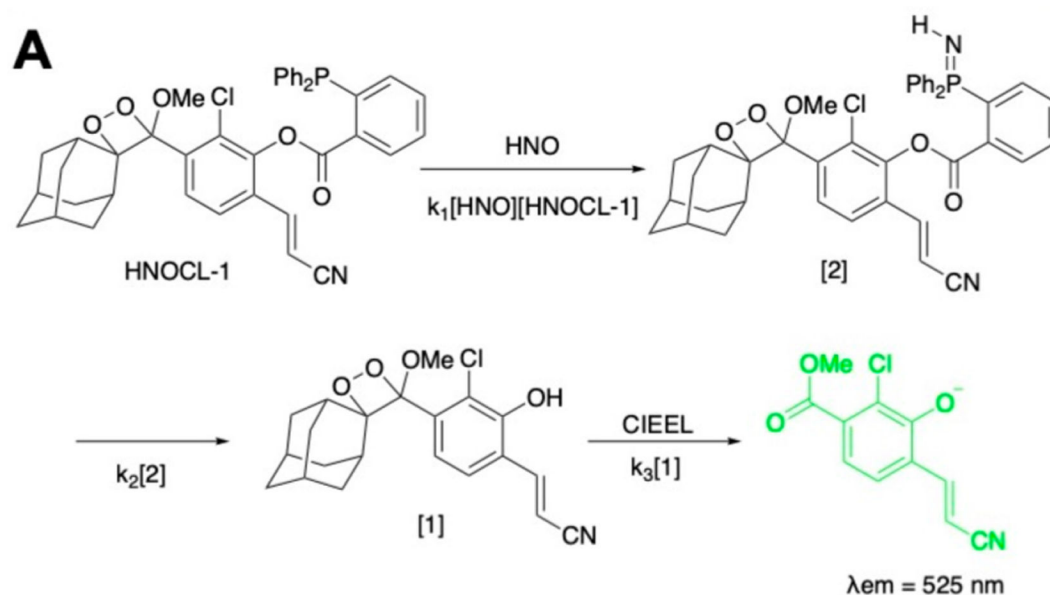


**Figure 8.** Ratiometric chemiluminescence imaging of pH in live mice using Ratio-pHCL-1. (A) Structure and chemiluminescence sensing mechanism of Ratio-pHCL-1. (B) Chemiluminescence images of Ratio-pHCL-1 after intraperitoneal injection into mice using 580 and 540 nm filters. (C) Ratio of the photon flux of the images in (B). Adapted with permission from ref 4. Copyright 2020 American Chemical Society.





$$[\text{HNO}] = 1/(k_1[\text{HNOCL-1}]) (k_3[1] + d[1]/dt)$$

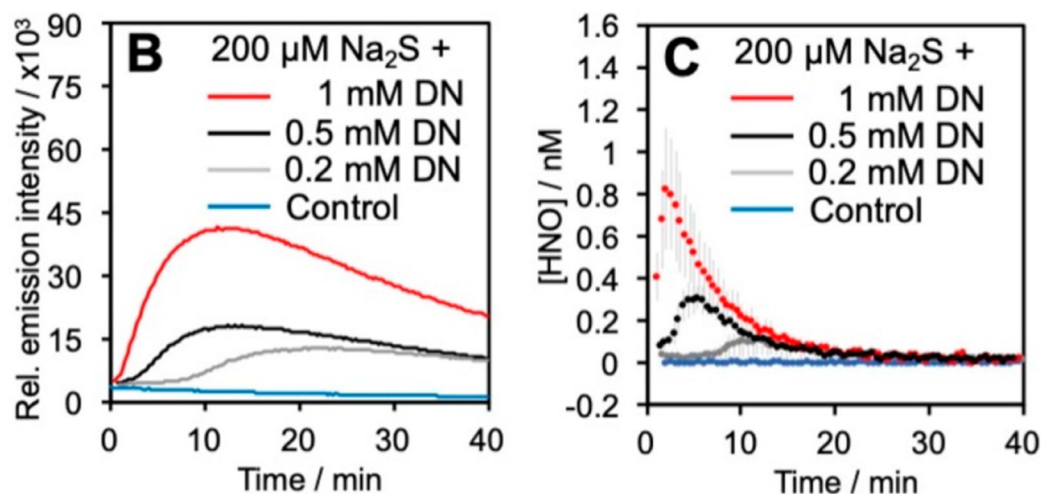


**Figure 9.**

Kinetics-based quantification of HNO. (A) Structure and mechanism of HNO detection with HNOCL-1. The rate equation gives the concentration of HNO in terms of [1], which is proportional to the chemiluminescence emission intensity. (B) Chemiluminescence emission intensity from HNO formed by the reaction of  $\text{H}_2\text{S}$  with nitric oxide produced from DEA NONOate (DN). (C) Conversion of the data in (B) into [HNO] using the derived equation. Adapted with permission from ref 3. Copyright 2019 Wiley-VCH GmbH, Weinheim.

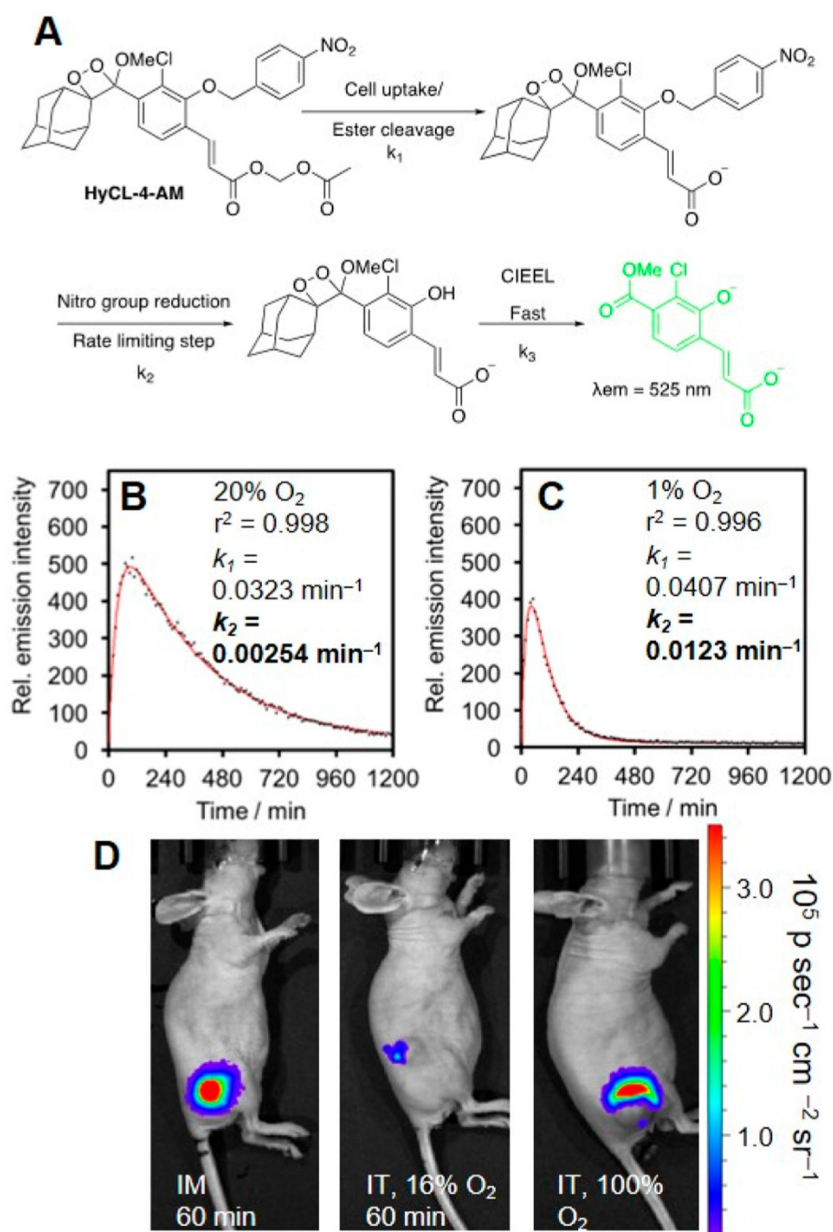


**Figure 10.** Kinetics-based hypoxia imaging with HyCL-4-AM. (A) Structure of HyCL-4-AM and model for cellular hypoxia sensing. (B, C) Kinetic fitting of the luminescence of HyCL-4-AM in A549 cells under (B) 20% O<sub>2</sub> and (C) 1% O<sub>2</sub>. (D) Comparison of HyCL-4-AM response in mice using an intramuscular (IM) injection, intratumoral (IT) injection at 16% O<sub>2</sub>, or intratumoral (IT) injection at 100% O<sub>2</sub>. Adapted with permission from ref 76. Copyright 2019 American Chemical Society.

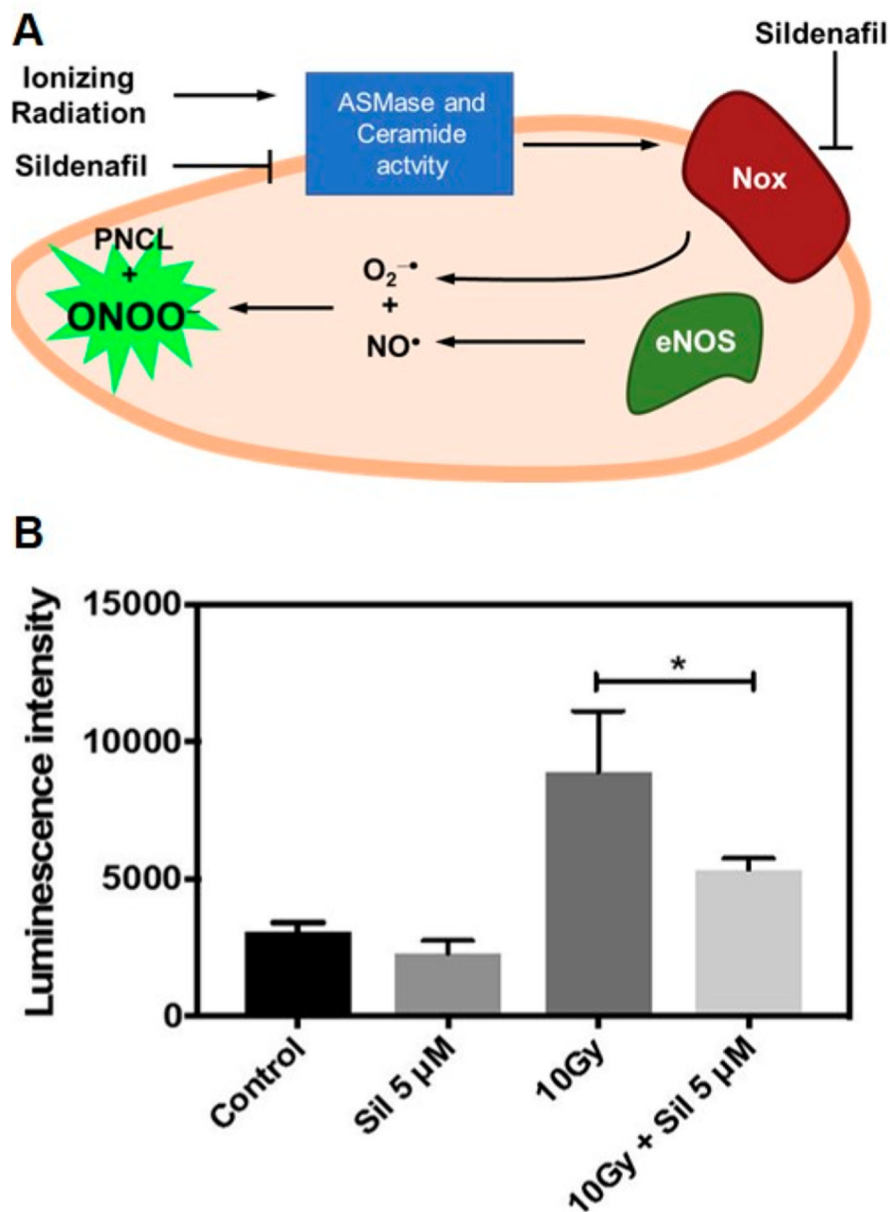


**Figure 11.** Measuring ONOO<sup>-</sup> in bovine aortic endothelial cells in response to radiation therapy. (A) Pathway of ONOO<sup>-</sup> production in radiation therapy and inhibition with sildenafil. (B) Luminescence response from PNCL in cells treated with vehicle control (Control), sildenafil (Sil 5 μM), radiation (10Gy), and radiation and sildenafil (10Gy + Sil 5 μM). Adapted with permission from ref 77. Copyright 2019 Elsevier.

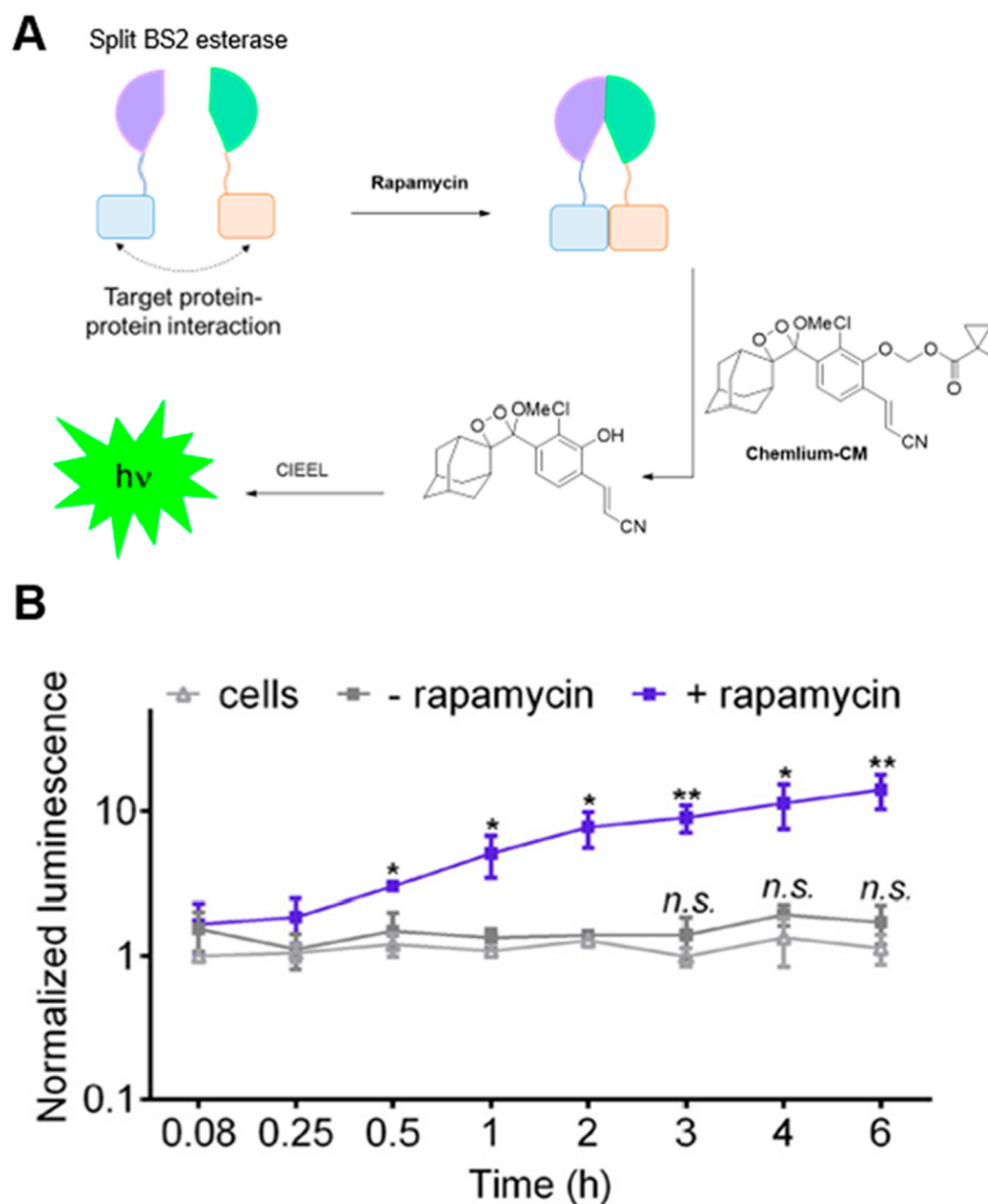


**Figure 12.**

Application of triggered chemiluminescence in a split-esterase system. (A) Chemilum-CM chemiluminescence can be activated by rapamycin-mediated split esterase assembly. (B) Chemiluminescence emission from Chemilum-CM in cells with or without rapamycin. Adapted with permission from ref 81. Copyright 2019 American Chemical Society.

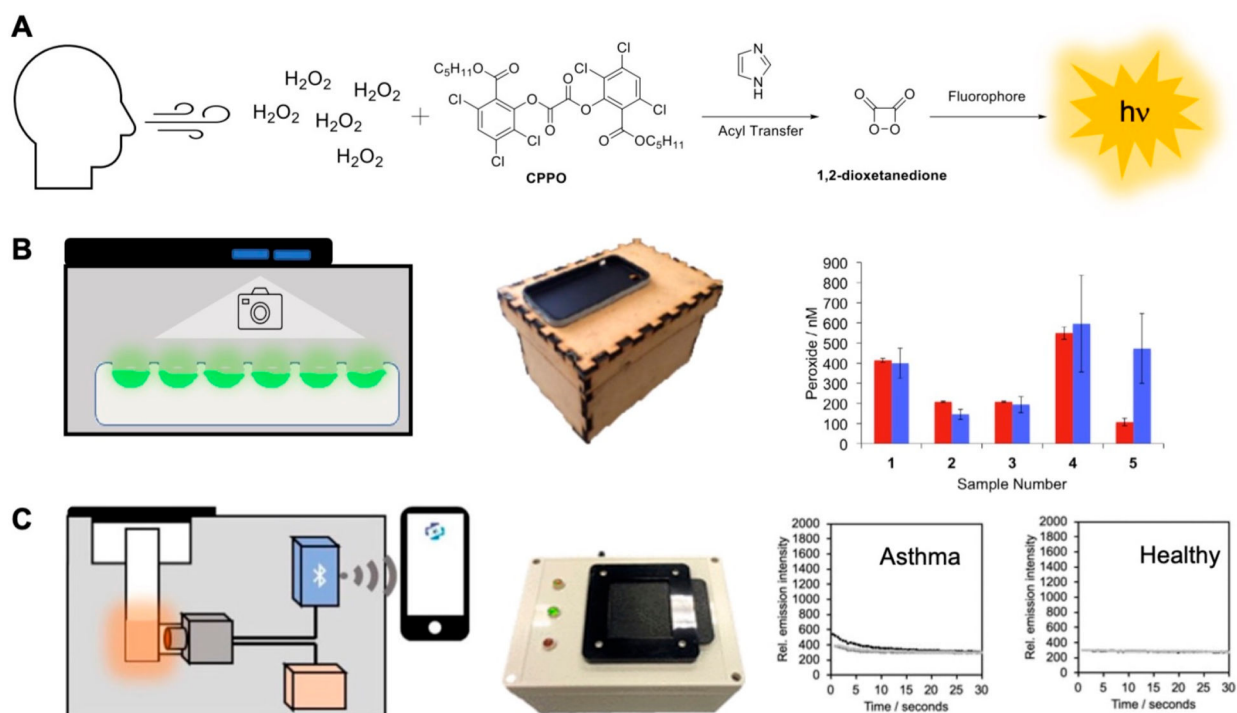


**Figure 13.** Chemiluminescence measurement of  $\text{H}_2\text{O}_2$  in human exhaled breath condensate. (A) Peroxyoxalate chemiluminescence assay for  $\text{H}_2\text{O}_2$  detection. (B) A smartphone was integrated to a wooden crafted dark box. Measurements in human exhaled breath condensate were validated versus the fluorescent Amplex Red assay. Adapted with permission from ref 82. Copyright 2016 Elsevier. (C) The BioSense 2.0 Laboratory Module was used to measure  $\text{H}_2\text{O}_2$  concentrations in asthma patients and healthy volunteers in the John Peter Smith Hospital.<sup>83</sup> Adapted with permission from ref 83. Copyright 2020 American Chemical Society.

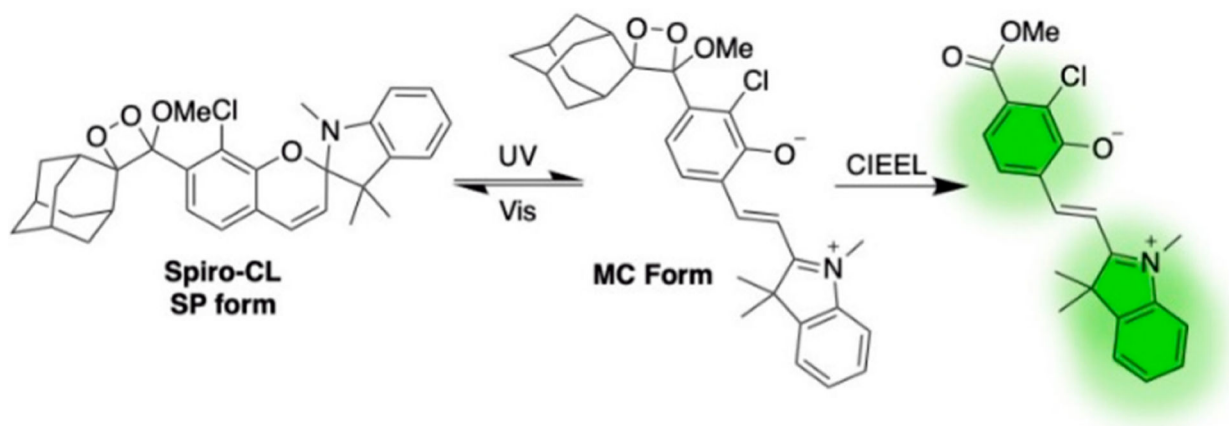
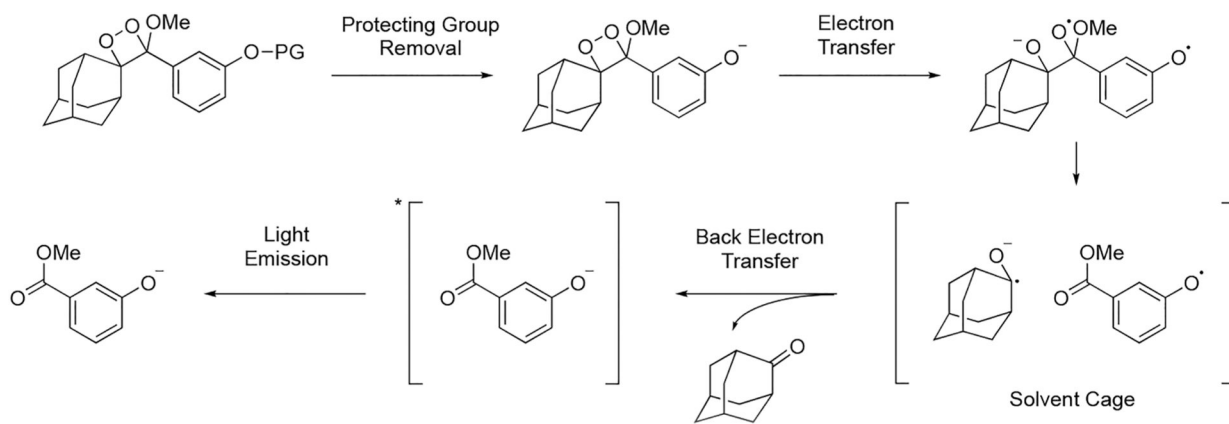
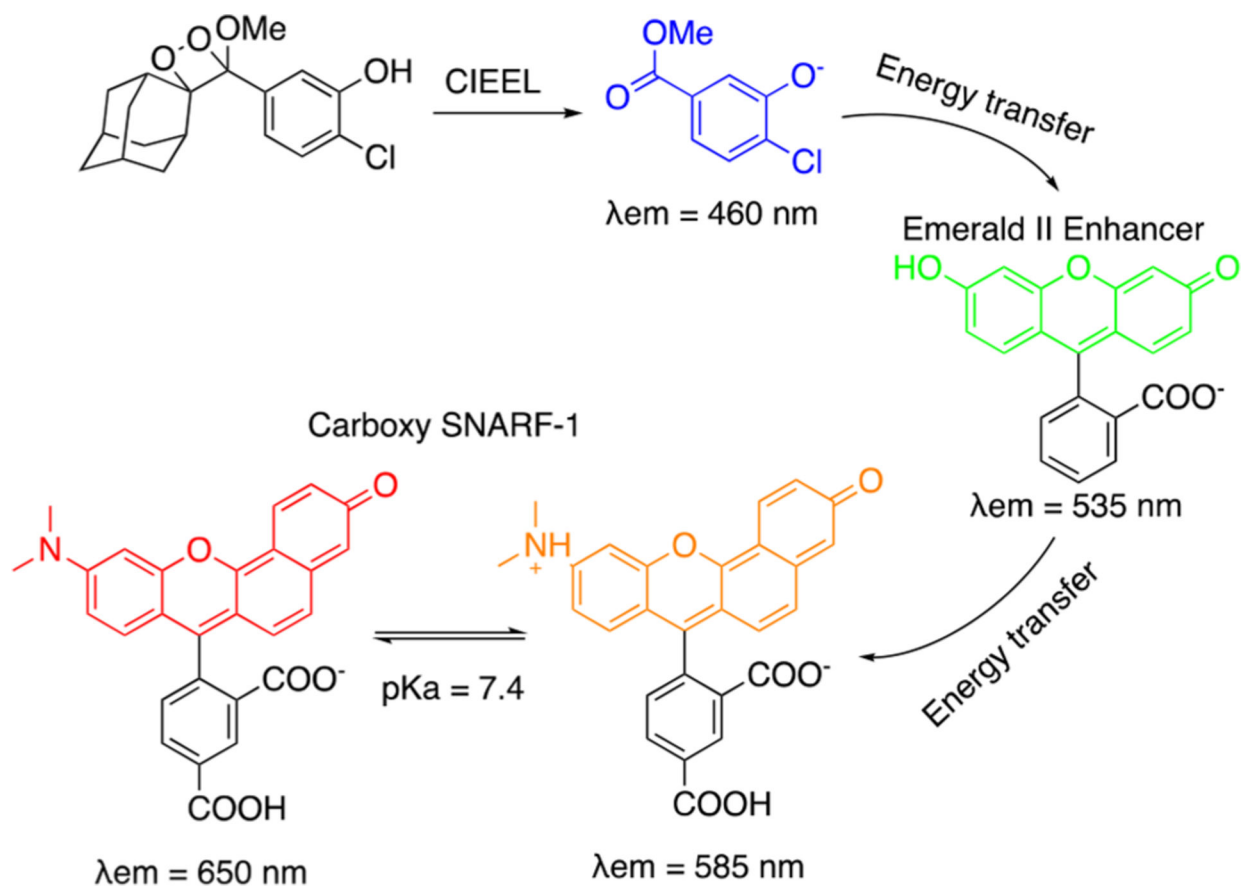


**Figure 14.**  
Photoswitchable chemiluminescent 1,2-dioxetane Spiro-CL.



**Scheme 1.**  
CIEEL Mechanism for Analyte-Triggered Chemiluminescence of 1,2-Dioxetanes



**Scheme 2.**  
 Ratiometric Chemiluminescence pH Imaging Using Chemiluminescence Energy Transfer to Carboxy SNARF-1



Table 1.

## Chemiluminescent 1,2-Dioxetane Probes for Detection of Biological Analytes

probe	analyte	enhancer	$\lambda_{em}$ (nm)	expt studies	quantification
CHS-1	H <sub>2</sub> S	Emerald II	545	<i>in vitro</i>	
CHS-2	H <sub>2</sub> S	Emerald II	545	<i>in vitro</i>	
CHS-3	H <sub>2</sub> S	Emerald II	545	<i>in vitro</i> , in cells, <i>in vivo</i>	
dioxetane + SNARF	pH	Sapphire II, Emerald II	460, 585, 650	<i>in vitro</i>	ratiometric
HNOCL-1	HNO		525	<i>in vitro</i> , in cells, <i>in vivo</i>	kinetics-based
HyCL-1	O <sub>2</sub>	Emerald II	455, 545	<i>in vitro</i>	
HyCL-2	O <sub>2</sub>	Emerald II	455, 545	<i>in vitro</i> , <i>in vivo</i>	
HyCL-3	O <sub>2</sub>		525	<i>in vitro</i>	
HyCL-4-AM	O <sub>2</sub>		516	<i>in vitro</i> , in cells, <i>in vivo</i>	kinetics-based
PNCL	ONOO <sup>-</sup>		525	in cells	
Ratio-pHCL-1	pH		530, 580	<i>in vitro</i> , <i>in vivo</i>	ratiometric